

**ANALYSIS OF HEAT TRANSFER RATE OF WAVY FINS ON A HORIZONTAL
BASE**

BY

**OKON, Joshua Oyosuhu
MEng/SEET/2017/7132**

**DEPARTMENT OF MECHANICAL ENGINEERING
FEDERAL UNIVERSITY OF TECHNOLOGY, MINNA**

SEPTEMBER, 2021

ABSTRACT

Fins are extended surfaces which help to increase the heat transfer rate from surfaces and help to reduce the temperature of the surface by increasing surface area. The application of the use of fins as heat sinks in device requires an additional space, which in most heat producing devices are not usually available. The aim of this study is to minimize the problem of increased space and weight usually associated with the use of finned heat sink, as well as achieving increased heat transfer rate in many electronic and mechanical devices, during system thermal design. As a means of tackling the problem of additional space and increased weight associated with the use of extended surfaces (fins), a numerical study to solve the 3-D forms of the continuity, momentum and energy equations for several configurations of a fin array was carried out based on Computational Fluid Dynamics (CFD) using Solidworks 2018 commercial version, to analyze the convection heat transfer in wavy fin protruding from a horizontal base. The critical parameters of the configurations examined are fin spacing, wavelength, and height. The fin thickness and length are fixed. The fin spacing ranged from (10.85mm to 28mm), fin wavelength (7mm to 10mm), fin height (15mm to 35mm). The fin thickness (3mm) and fin length (95mm) were fixed. Based on the simulation results, it was discovered that wavy fins have effective convective heat transfer rate and is based on the fin height, wavelength and fin spacing. And comparatively the heat transfer rate of any given wavy fin array and it stretched length is about 9% less. It was also observed that the convective heat transfer rate for the wavy fin array is greater than that of the straight rectangular fin array of the same fin height and fin spacing by about 28% at higher base-to-ambient temperature difference. When the wavy fin effective or elliptical length was stretched into a straight fin, and their heat transfer rate compared, the stretched fin occupied additional height of about 43%. This implies that the use of a wavy fin array instead of the rectangular straight fin array eliminates fin additional space to the system design by 43%. Therefore, wavy fins could be recommended for heat sink design where space, weight and size are of ultimate consideration.

TABLE OF CONTENT

| Contents | pages |
|-------------------------------------|--------------|
| Cover page | |
| Title page | i |
| Declaration | ii |
| Certification | iii |
| Acknowledgements | iv |
| Abstract | vi |
| Table of Content | vii |
| List of Tables | x |
| List of Figures | xi |
| List of Symbols and abbreviations | xv |
| CHAPTER ONE | |
| 1.0 INTRODUCTION | 1 |
| 1.1 Background of the Study | 1 |
| 1.2 Statement of the Problem | 3 |
| 1.3 Aim and Objectives of the Study | 4 |
| 1.4 Justification of the Study | 5 |
| 1.5 Scope and Delimitation Study | 5 |
| CHAPTER TWO | |
| 2.0 LITERATURE REVIEW | 6 |
| 2.1 Introduction | 6 |
| 2.2 Heat Transfer | 6 |

| | | |
|----------------------|---|-----------|
| 2.2.1 | Conduction | 7 |
| 2.2.2 | Convection | 9 |
| 2.2.3 | Radiation | 10 |
| 2.3 | Extended surfaces | 11 |
| 2.4 | Analytic Solution of Extended Surfaces | 18 |
| 2.5 | Fin Performance | 19 |
| 2.5.1 | Fin Effectiveness | 20 |
| 2.5.2 | Fin Efficiency | 21 |
| 2.5.3 | Overall Surface Efficiency | 21 |
| CHAPTER THREE | | |
| 3.0 | MATERIALS AND METHODS | 23 |
| 3.1 | Material and Configuration Geometry | 23 |
| 3.2 | Theoretical Analysis of Heat Transfer | 27 |
| 3.3 | Mathematical Theories/Governing Equations | 28 |
| 3.4 | Simulation Procedure | 29 |
| 3.4.1 | Geometrical Modeling of the Fin Array | 29 |
| 3.4.2 | Determining the Computational Domain | 30 |
| 3.4.3 | Material Selection | 30 |
| 3.4.4 | Selection of Boundary Conditions | 30 |
| 3.4.5 | Meshing of the Fin Array Solid | 31 |
| 3.4.6 | Results | 32 |
| 3.5 | Validation of Simulation Result | 32 |

CHAPTER FOUR

| | | |
|---------------------|--------------------------------------|-----------|
| 4.0 | RESULTS AND DISCUSSIONS | 33 |
| 4.1 | Introduction | 33 |
| 4.2 | Results and Analysis | 33 |
| CHAPTER FIVE | | |
| 5.0 | CONCLUSION AND RECOMMENDATION | 52 |
| 5.1 | Conclusion | 52 |
| 5.2 | Recommendation | 53 |
| REFERENCES | | 54 |
| APPENDIX A | | 67 |
| APPENDIX B | | 61 |

LIST OF TABLES

| Tables | | Page |
|-----------|--|------|
| Table 3.1 | Dimension of Fin Configuration | 24 |
| Table 3.2 | Dimension of Compared Fin Configuration of Wavy, Stretched and Straight Fin Array | 25 |
| Table 3.3 | Simulation and Boundary Parameters | 31 |
| Table 3.4 | Fin Array Configuration Geometry | 32 |
| Table 4.1 | Experimental Versus Simulation Heat Transfer Rate Result at $\Delta T = 15^{\circ}\text{C}$ | 39 |

LIST OF FIGURES

| Figures | Page |
|---|------|
| 2.1 Diagram Showing Heat Transfer by Conduction | 8 |
| 2.2 Diagram Showing Convection Heat Transfer in Boiling Liquid | 10 |
| 2.3 Diagram Showing the Combined Heat Transfer by Conduction, Convection and Radiation | 12 |
| 2.4 Applications of Extended Surfaces (Fins). | 13 |
| 2.5 Heat Transfer Fin Types | 15 |
| 2.6 Fin Patterns | 16 |
| 2.7 Overall Performance of Fin Array | 23 |
| 3.1 Wavy Fin Configuration Geometry | 26 |
| 3.2 Wavy Fin Configuration Geometry Views | 27 |
| 4.1 Meshing of Fin Array | 34 |
| 4.2a Surface Plot Showing the Solid Temperature of Wavy Fin Array of $H = 25$ mm, $s = 9.9$ mm at Wall Temperature of 45°C | 34 |
| 4.2b Surface Plot Showing the Solid Temperature of Rectangular Fin Array Geometry at Wall Temperature of 120°C | 35 |
| 4.2c Surface Plot Showing the Solid Temperature of Wavy Fin Array of $H = 25$ mm, $s = 7.3$ mm at Wall Temperature of 45°C | 35 |
| 4.3. Cut Plot of Fluid Temperature | 36 |
| 4.4 Comparison of Heat Transfer by Experiment and Simulation | 37 |
| 4.5 Variation of Convection Heat Transfer Rate with Fin Spacing at A Fin Height of $H = 15$ mm and at a Fin Length of $L = 95$ and $\lambda = 7$ mm | 38 |
| 4.6 Variation of Convection Heat Transfer Rate with Fin spacing at a Fin Height of $H = 25$ mm and at a Fin Length of $L = 95$ mm and $\lambda = 7$ mm | 39 |
| 4.7 Variation of Convection Heat Transfer Rate with Fin spacing at a Fin Height of $H = 35$ mm and at a Fin Length of $L = 95$ mm and $\lambda = 7$ mm | 39 |
| 4.8 Variation of Convection Heat Transfer Rate with Fin spacing at a Fin | 40 |

| | | |
|------|---|----|
| | Height of $H = 15\text{mm}$ and at a Fin Length of $L = 95$ and $\lambda = 10\text{ mm}$ | |
| 4.9 | Variation of Convection Heat Transfer Rate with Fin spacing at a Fin | 40 |
| | Height of $H = 25\text{ mm}$ and at a Fin Length of $L = 95\text{ mm}$ and $\lambda = 10\text{ mm}$ | |
| 4.10 | Variation of Convection Heat Transfer Rate with Fin spacing at a Fin | 41 |
| | Height of $H = 35\text{ mm}$ and at a Fin Length of $L = 95\text{ mm}$ and $\lambda = 10\text{ mm}$ | |
| 4.11 | Variation of Convection Heat Transfer Rate with Fin Height at a Fin | 41 |
| | Spacing of $s=7.3\text{mm}$ and at a Fin Length of $L=95\text{mm}$ and $\lambda = 7\text{ mm}$ | |
| 4.12 | Variation of Convection Heat Transfer Rate with Fin Height at a Fin | 42 |
| | Spacing of $s=9.9\text{mm}$ and at a Fin Length of $L=95\text{mm}$ and $\lambda = 7\text{ mm}$ | |
| 4.13 | Variation of Convection Heat Transfer Rate with Fin Height at a Fin | 42 |
| | Spacing of $s=14.2\text{mm}$ and at a Fin Length of $L=95\text{mm}$ and $\lambda = 7\text{ mm}$ | |
| 4.14 | Variation of Convection Heat Transfer Rate with Fin Height at a Fin | 43 |
| | Spacing of $s=14.2\text{mm}$ and at a Fin Length of $L=95\text{mm}$ and $\lambda = 7\text{ mm}$ | |
| 4.15 | Variation of Convection Heat Transfer Rate with Fin Height at a Fin | 43 |
| | Spacing of $s=7.3\text{mm}$ and at a Fin Length of $L=95\text{mm}$ and $\lambda = 10\text{ mm}$ | |
| 4.16 | Variation of Convection Heat Transfer Rate with Fin Height at a Fin | 44 |
| | Spacing of $s=9.9\text{mm}$ and at a Fin Length of $L=95\text{mm}$ and $\lambda = 10\text{ mm}$ | |
| 4.17 | Variation of Convection Heat Transfer Rate with Fin Height at a Fin | 44 |
| | Spacing of $s=14.2\text{mm}$ and at a Fin Length of $L=95\text{mm}$ and $\lambda = 10\text{ mm}$ | |
| 4.18 | Variation of Convection Heat Transfer Rate with Fin Height at a Fin | 45 |
| | Spacing of $s=14.2\text{mm}$ and at a Fin Length of $L=95\text{mm}$ and $\lambda = 10\text{ mm}$ | |
| 4.19 | Variation of Convection Heat Transfer Rate with Base-to-Ambient | 46 |
| | Temperature Difference at $H=15\text{ mm}$, $L=95\text{ mm}$ and $\lambda = 7\text{ mm}$ | |
| 4.20 | Variation of Convection Heat Transfer Rate with Base-to-Ambient | 47 |
| | Temperature Difference at $H=25\text{ mm}$, $L=95\text{ mm}$ and $\lambda = 7\text{ mm}$ | |
| 4.21 | Variation of Convection Heat Transfer Rate with Base-to-Ambient | 47 |
| | Temperature Difference at $H=35\text{ mm}$, $L=95\text{mm}$ and $\lambda = 7\text{ mm}$ | |
| 4.22 | Variation of Convection Heat Transfer Rate with Base-to-Ambient | 48 |
| | Temperature Difference at $H=15\text{ mm}$, $L=95\text{ mm}$ and $\lambda = 10\text{ mm}$ | |
| 4.23 | Variation of Convection Heat Transfer Rate with Base-to-Ambient | 48 |
| | Temperature Difference at $H=25\text{ mm}$, $L=95\text{ mm}$ and $\lambda = 10\text{ mm}$ | |
| 4.24 | Variation of Convection Heat Transfer Rate with Base-to-Ambient | 49 |
| | Temperature Difference at $H=35\text{ mm}$, $L=95\text{mm}$ and $\lambda = 10\text{ mm}$ | |

LIST OF ABBREVIATIONS/SYMBOLS

| Symbols | Definitions/Description | Units |
|-----------------|---|-------------|
| A_c | Cross sectional area of convective surface | m^2 |
| A | Total convective surface area | m^2 |
| H | Fin height | m |
| k | Thermal conductivity | $W/(mK)$ |
| L | Fin length | m |
| S | Fin spacing | m |
| t | Fin thickness | m |
| T_a | Ambient temperature | K |
| T_w | Wall temperature | K |
| T_b | Base plate temperature | K |
| ΔT | Base- ambient temperature difference | K |
| h | Convection heat transfer coefficient | $W/(m^2 K)$ |
| Q | Rate of conduction heat transfer | W |
| t_f | Fluid temperature | K |
| t_s | Surface temperature | K |
| σ | Stefan-Boltzman constant and is equal the value $5.67 \times 10^{-8} W/m^2 K^4$ | |
| ε_f | Fin efficiency | |
| q_f | Fin heat transfer rate | W |
| θ_b | Base temperature difference in | K |
| R_t | Fin thermal rsistance | |

| | | |
|-----------|----------------------------|---|
| η_f | Efficiency of fin | |
| η_o | Overall surface efficiency | |
| λ | Wavelength of wavy fin | m |
| N | Number of fins | |
| L_e | Elliptical length | m |
| kW | Fin base width | m |

LIST OF APPENDICES

| | |
|------------|--|
| APPENDIX A | Tables of Simulation results |
| APPENDIX B | Orthographic drawing of fin configuration geometry |
| APPENDIX C | Isometric models of fin configurations |

CHAPTER ONE

1.0

INTRODUCTION

1.1 Background of the Study

One common occurrence in electrical and electronic components is the generation of heat due to its operations. This sometimes leads to overheating of an electrical system (May and Almubarak, 2017). The end effects of this overheating if not effectively dissipated out of the system may give rise to malfunctioning and sometimes total damage of the system. The heat generated within a system must be dissipated to its surrounding in order to maintain the system at its recommended working temperatures and functioning effectively and reliably.

Convective heat transfer therefore is usually used to dissipate heat generated using either or all of the following ways:

- i. Increasing the gradient of temperature between the surface and the ambient air using a fan or an air conditioner to lower the temperature of the environment (or ambient temperature).
- ii. Increasing the heat transfer coefficient which is usually achievable on creating proper conditions of forced flow over the surface.
- iii. By increasing the surface area of the electronic or mechanical system.

Bhambareet *al.*, (2016) noted that the first two ways may not be feasible but increasing the surface area can rather be more economical in enhancing the surface heat transfer rate. Therefore extended surfaces as a result of fins attachments are used to increase the surface area of the electronic and mechanical systems and thereby increase the rate of heat transfer

from the surface. The heat transfer rate from the finned systems to the external ambient atmosphere as researched by Yazicioğlu, (2005), may be determined using the convection and radiation heat transfer mechanism, but the effect of radiation contribution in total heat transfer rate is quite low due to low emissivity values of fin materials (Yardiet al. 2017). An improvement in heat transfer rate employing the use of extended surfaces like fins can be achieved by optimum configuration of fin array, which increases the surface area and as such the fin configuration parameters, such as fin spacing, fin length, height as well as fin shape which are very essential. Bhambare *et al.* (2016) noted that a closely packed fin array has greater surface area thereby apparently effect more heat transfer rate, though may result in reduction rate owing to the reduction in heat transfer coefficient. In contrast wide spacing between the fins which implies reduced surface area could results in greater heat transfer coefficient, thereby implying low heat transfer rate.

Extended surfaces according to Mathiazhagan and Jayabharathy, (2014) are specially used to enhance heat transfer rate between a solid and an adjoining fluid. The heat transfer from fins is simply a combined effort of both conduction and convection heat transfer and temperature distribution along the geometry of the material (Incropera *et al.*, 2007).

Extended surfaces are numerously applied as heat sinks or heat exchangers in electrical or electronic systems such as; air conditioner, refrigerators, power transformers, plants, as well as radiators in cars, engine cylinders, CPU heat sink, heat exchangers in power plants, and others.

Fins are usually in different configurations. Incropera *et al.*, (2007) explained four distinct fin configurations as shown in Figure 2.5. These fins are; straight fin having uniform cross section area, straight fin with non-uniform cross sectional area, annular fin, and pin fin. A

straight fin is an extended surface attached to a plane wall, which could be of uniform or non-uniform cross sectional area, and having varying height distance in x - direction from the wall. An annular fin that is attached to the circumference of a cylinder and its cross section varies from the cylinder wall. A pin fin or spine is an extended surface of circular cross section. It could be of uniform and non-uniform cross section. For any application, selection of a particular fin configuration may be dependent upon space, weight, manufacturing, and cost considerations. Other considerations may be the extent to which the fins are capable of reducing the surface convection coefficient and increase the pressure drop that is associated with the flow over the fins. On the basis of weight and space that extended surfaces may add to electronic and mechanical system, the study of the heat transfer rate of a wavy fin has become so necessary to check the additional space and weight fins may cause to electronic and mechanical systems.

1.2 Problem Statement

The operation of several engineering system give rise to heat generation within the system. This unwanted heat may lead to severe overheating problems and could at times give rise to system failure or malfunctioning. According to May and Almubarak, (2017), most engineering systems are designed and built to withstand a certain amount of heat energy. Therefore the additional heat generated during the operation of this systems has to be transferred to its environment or surroundings so as to keep the system at its recommended working temperatures as well as functioning effectively and reliably (Yazicioğlu, 2005). In most applications the transfer of heat energy must take place as rapidly as possible (Miller, 1967). In order to achieve this, several researches have been carried out on the use of thermal systems with effective emitters as extended surfaces otherwise called fins,

especially when combined surface conductance is low with different materials to establish their heat dissipative performance. These fins have been helpful in solving the problem of overheating in electronic and mechanical systems.

The fact remains that the integration of finned heat sink or extended surfaces requires additional space which is usually not required because of the possibility of increasing the weight of the system as well as the production cost associated with more material usage. Therefore this increase in space and weight has become a major problem in many engineering thermal system design in this era where reduction in size and weight and even miniaturizing of electronic system is becoming a designing goal. This study therefore seeks to investigate and analyze the heat transfer rate of wavy fin with several configurations to check the problem of addition space and increase size in electronic and mechanical system design.

1.3 Aim and Objectives of the Study

The aim of this study is to analyze the rate of heat transfer in wavy fin shape array. The following are its specific objectives:

- i. To apply the appropriate governing equation to generate the flow pattern of temperature fields around the different configurations of the fin examined.
- ii. To analyze the flow of temperature fields to obtain the heat transfer rates of the configurations
- iii. To determine the performance of a straight fin and wavy fin by comparing their heat transfer rates.

1.4 Justification of the Study

The problem of overheating in engineering systems arising from its operation, as well as the design issues encountered by Thermal Engineers to dissipate these generated heat in a steady, fast and in a consistent manner has compelled this research study. The significance of this study is such that it will enable the design engineers to understand the effect of finned sink or extended surface shape and configuration on the heat transfer rate.

It may also be of help to the design engineer in the choice of fin orientation and shape in carrying out his thermal design to overcome the thermal design problems of limited space and as well as size.

1.5 Scope and Limitations of the Study

This research used numerical simulation approach to analyze the rate of heat transfer in an extended surface or fin of combined geometry, specifically wavy fin geometry. Even though both forced and free convection could be used for the analysis, this work is limited to steady-state free convection heat transfer. Lastly, due to the very low emissivity of aluminum material used in this analysis, radiation heat transfer is neglected. Therefore, only the heat transfer rate between the surface and ambient or environment air was considered using convection heat transfer and a steady-state natural or free convection analysis.

CHAPTER TWO

2.0 LITERATURE REVIEW

2.1 Introduction

Over the years, the quest for effective heat energy transfer from engineering systems to overcome the thermal problems of overheating has led to several experimental and numerical research studies on the best design of extended surfaces (fins) to achieve optimum heat transfer rate. Several studies have been done on the optimizing fin geometry, investigation into the rate of heat transfer on different fin shapes, and several other studies regarding extended surfaces for effective or optimal heat transfer. This chapter will be reviewing some of those already made studies on extended surfaces especially that of a wavy finned heat sinks and heat exchangers.

2.2 Heat Transfer

Heat is basically a form of energy which must be transferred as a result of the interaction of a system and its surroundings (Bakaleet *et al.*, 2016). Several authors have emerged with several definitions of heat transfer, but all of these definitions have the same meaning.

Incropera *et al.*, (2007) defined heat transfer as the thermal energy in transition due to spatial temperature difference. Similarly, Long and Szyma, (2009) defined heat transfer as energy in transition due to temperature differences. Heat transfer is also defined as the science that deals with the determination of the rate of heat energy transfer. Rajput, (2003), in his book defined heat transfer as the transmission of energy from one region to another as a result of temperature gradient.

From the various definitions of heat transfer cited above, it can be deduced that heat transfer cannot occur if there is no temperature difference. In other words, heat transfer will not take place between two medium at the same temperature. Just as the voltage difference is the driving force for electrical current to flow, so is temperature difference the driving force for heat transfer. Therefore the rate of heat transfer in a certain direction is a function of the magnitude of the temperature difference or gradient. The higher the temperature gradient, the higher the rate of heat transfer(Rajput, 2003).

Heat transfer is achieved in three different ways otherwise known as mode of heat transfer. These are; heat transfer by conduction, convection and radiation.

2.2.1 Conduction

Conduction refers to the transfer of heat from one part of a substance to another part of the same substance or from one substance to another in physical contact with it without appreciable displacement of molecules (Rajput, 2003).

Heat conduction in solid is by two mechanism; lattice vibration and by transport of free electrons(that is, energy flux in the direction of decreasing temperature is made available by these free electrons).

Bearing in mind the concept of atomic and molecular activities, conduction may be viewed as the transfer of energy from more energetic to the less energetic particles of a substance due to interaction between the particles (Incropera *et al.*, 2007).

An empirical based law used to explain heat conduction is the Fourier's Law of heat conductionThis law states that "the rate of heat flow through a simple homogeneous solid is directly proportional to the area of the section at right angle to the direction of heat flow

and to the change of temperature with respect to the length of the part of the flow”(Eastop and McConkey, 2006).

Mathematically,

$$Q \propto A \frac{dT}{dx} \quad 2.1$$

$$Q = -KA \frac{dT}{dx} \quad 2.2$$

(Eastop and McConkey, 2006)

Where K is constant of proportionality (W/mK) called thermal conductivity, which is uniformall through the conducting material (Rajput, 2003). The negative sign recognizes the direction for flow of heat from high to low temperature.

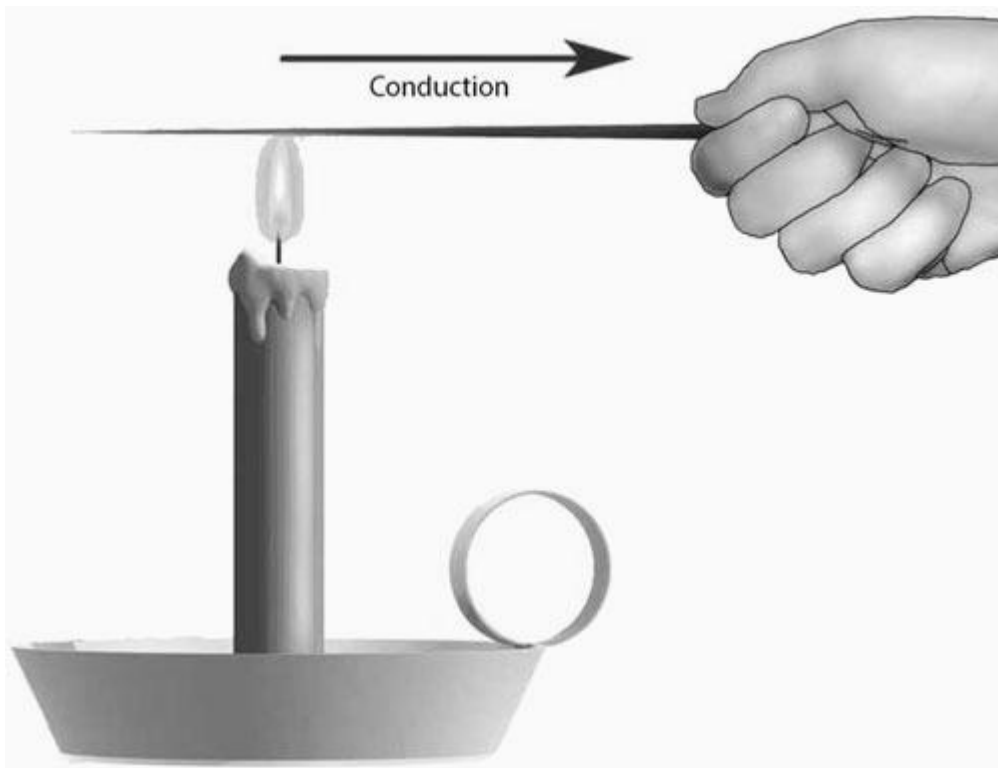


Figure 2.1: Diagram showing heat transfer by conduction. (www.science4fun.info.)

2.2.2 Convection

Convection heat transfer occurs due to molecular motion and bulk fluid motion (Long and Sayma, 2009). Convection as defined by Rajput, (2003), is the transfer of heat within a fluid by mixing of one portion of fluid with another. It is a mode of energy transfer between a solid surface and the adjacent liquid or gas that is in motion. Convection is possible only in fluid medium and is basically a function of the transport of the medium (Bakale et al., 2016). Two categories of convection heat transfer exist; natural convection and forced convection. Natural convection takes place as a result of density differences associated with temperature change. In other words, the fluid flow is induced by buoyancy force. Yardi et al., (2017) noted that if the fluid is made to forcefully flow over the surface by the use of fan, pumps, bellows and others, as an external means such convection is forced.

Newton's Law of Cooling prescribes the rate equation for convective heat transfer between surface and adjacent fluid as;

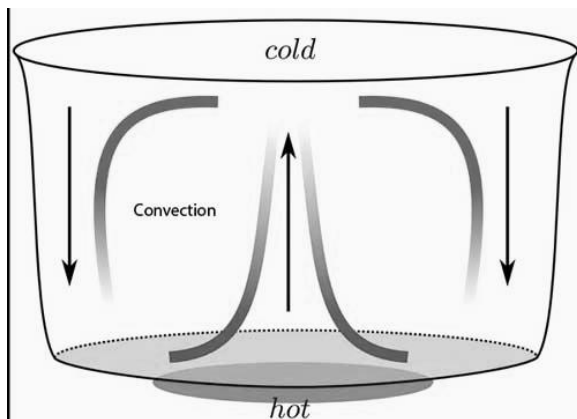


Figure 2.2: Diagram showing Convection heat transfer in boiling liquid (Rajput, 2003)

$$Q = hA (t_s - t_f) \quad (\text{Sahu et al. 2018}).$$

Where Q = rate of convective heat transfer,

A = surface area exposed to heat transfer

t_s = surface temperature

t_f = fluid temperature and

h = coefficient of convective heat transfer in $\text{W/m}^2\text{K}$

the coefficient of convective heat transfer (h) is a function of the nature of the fluid flow, geometry of the surface, prevailing thermal condition and the thermodynamic and transport properties (such as viscosity, density and surface heat)(Rajput, 2003).

2.2.3 Radiation

Radiation refers to the transfer of energy through space or matter by means other than conduction or convection(Long and Sayma, 2009). It is considered to be an electromagnetic wave quantum. Just as conduction and convection use media for heat transfer, radiant energy requires no medium for propagation but passes through vacuum. Thermal radiation belongs to the same family as visible light and behaves in the same fashion generally being reflected, refracted and absorbed.Long and Sayma, (2009) in his work affirmed that everybody unless at the absolute zero temperature will both emit and absorb energy by radiation.

An expression for the net transfer of energy from an idealized body (Black body) was put forward by Stefan Boltzmann Law, which states that “the emissive power of a black body is directly proportional to the fourth power of its absolute temperature”.

$$Q \propto T^4$$

$$Q = F\sigma A (T_2^4 - T_1^4) \quad 2.4$$

(Eastop and McConkey, 2006).

Where F is a factor that depends on the geometry and surface properties. And σ is called the Stefan-boltzman constant and is equal to the value $5.67 \times 10^{-8} \text{W/m}^2\text{k}^4$, and A is the radiating surface area in square meters, m^2 , T_1 and T_2 are the temperatures in degree kelvin, K see Figure 2.3.

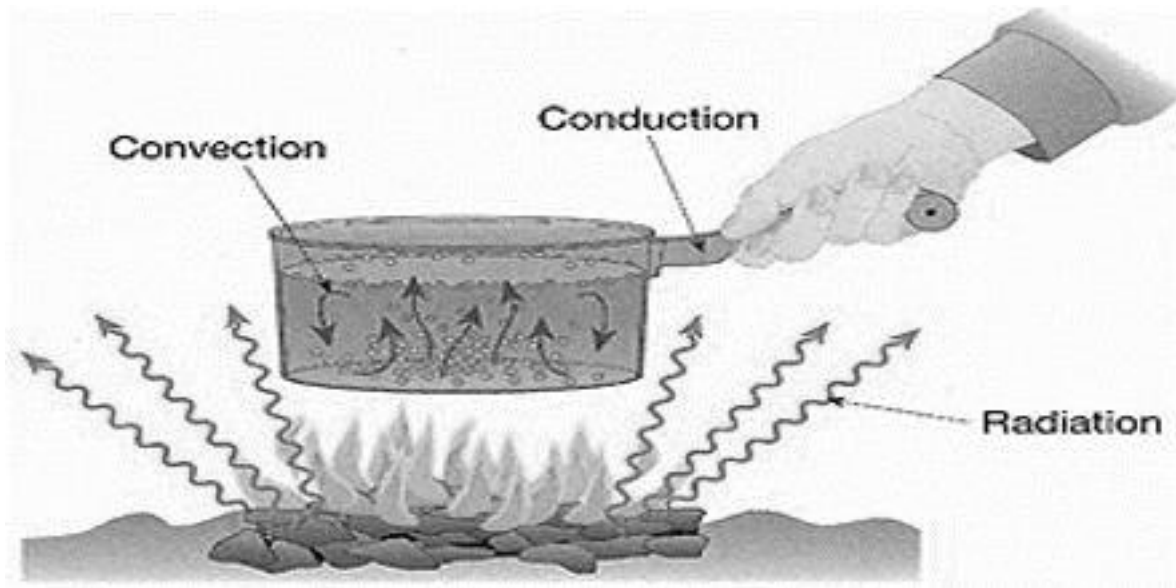


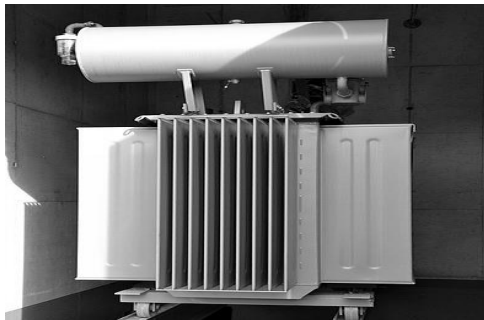
Figure 2.3: Diagram showing the combined heat transfer by conduction, convection and radiation (Rajput, 2003)

2.3 Extended Surfaces (Fins)

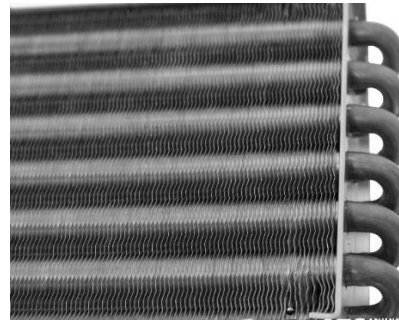
Fins are extended surfaces which help to increase the heat transfer from surface and help to reduce the temperature of the surface (Yardi *et al.*, 2017). Extended surfaces may exist in

several situations but are frequently used to enhance heat transfer by increasing the surface area available for convection (CuceandCuce, 2014).

Extended surfaces are numerous applied as heat sinks or heat exchangers in electrical or electronic systems such as; air conditioner, refrigerators, power transformers, plants, as well as radiators in cars, engine cylinder, CPU heat sink, exchangers in power plants, electric motors and pumps and others. Figure 2.4 shows examples of application of extended surfaces.



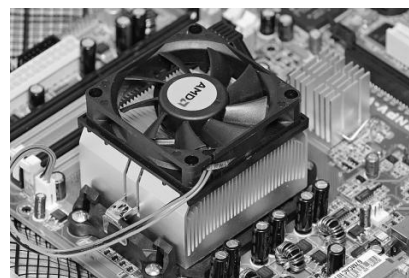
(a) Power transformer



(b) Car Radiator



(d) Electric motor



(c) Electronic chip board.

Figure 2.4: Applications of extended surfaces (fins)
(<https://autotechwestislip.com/maintaining-your-vehicle-cooling-system/>).

Extended surfaces used often to describe important special cases involving heat transfer by conduction within a solid, as well as heat transfer by convection and/or radiation from

boundaries or solid(Khosravy, n.d.). This extended surfaces are used as heat exchangers either alone or imbedded with tube.

Yazicioglu, (2005) observed that fins are thermal systems with effective emitters used to dissipate heat generated specially in modern electronic system thereby solving the problems of overheating. He further noted that in a bid to attain the desired rate of heat transfer with minimum amount of material, the overall combination of geometry and orientation of the finned surface is needed.

According to Lohar, (2014) natural convection cooling with the help of finned surfaces often offer an economical and trouble-free solution in different situations and that finned array on horizontal and vertical surface are used in a variety of engineering application to dissipate heat. Kang, (2012) cites Web, (1994) as noting that the purpose of fin is to increase the product of the surface area and heat transfer coefficient. Luet *al.*(2009) maintain that the only controlling variables in the hands of the designer are orientation and geometry of fins in order to maximize the heat transfer rate.

Based on the geometry of fins and the array for optimizing fin performance and the rate of heat transfer, geometries such as shape, thickness, height, length and spacing of fins are considered.

Incropera *et al.*, (2007) described different fin geometrical configurations to include straight fin with uniform cross section, annular fin, straight fin of non-uniform cross-section as well as pin fin. The above-mentioned fin types are depicted in the figures below.

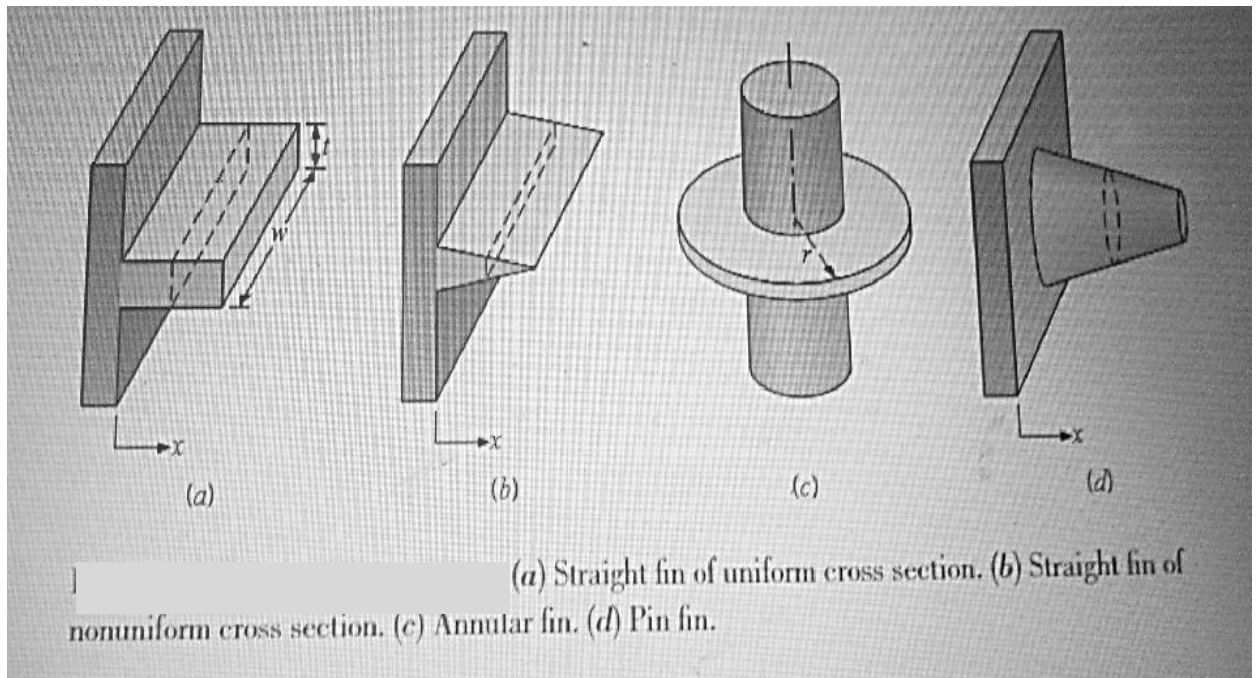
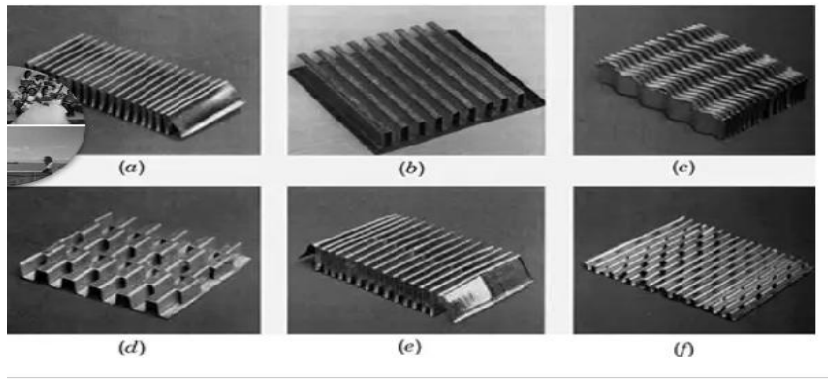


Figure 2.5: Heat transfer fin configurations. (Incropera *et al.*, 2007)

Moorthy *et al.*, (2018) conducted an experimental study using wavy, plain and rectangular-grooved fin in which it was concluded that the wavy fin has the ability to increase airflow on the heat exchange by enhancing and improving the air flow mixing thereby increase the heat transfer performance. In addition, Moorthy *et al.*, (2018) noted that wavy fin are cheap, reliable and easier to install. The researchers note that the waviness of a fin enhances heat transfer because wavy or sinusoidal fins has more surface area due to corrugation as well as promotes turbulence at bigger flows.



(a) Plain triangular fin; (b) plain rectangular fin; (c) wavy fin; (d) offset strip fin; (e) multi-louver fin; (f) perforated fin

Figure 2.6: Fin patterns (Erbay, *et al.*, 2017)

There exist several fin patterns, such as plate, louver, convex-louver and wavy fin pattern. Among these patterns, plate fin configuration is the most used fin pattern in heat exchanger application as a result of its simplicity, rigidity and economic factor (Bilir and Ilken, 2005).

Donget *al.*, (2013), in their experimental study of the air-side thermal hydraulic performance of wavy fin aluminum plate fin heat exchanger, established from their results obtained that the ratio of the fin amplitude and the wave length is the most important factor that affects the overall thermal hydraulic performance. In terms of the waviness of the finned heat sink, Wolf, *et al.*, (2006) maintained that it can be adjusted to increase the surface area, thereby resulting in positive impact on thermal performance. According to Nikamet *al.*, (2015), the wavy fin is remains one of the most used fin types in plate fin heat exchangers, especially where optimum heat transfer performance is required amidst tight pressure drop allowance. They further maintained that the wavy fin is a continuous surface with cross section shape similar to that of plain fins but with undulations in the flow direction. Though Borrajo-pérez and Reyes-fernández-de-bulnes, (2016) maintained that

further empirical testing is warranted for the evaluation of the effects of wavy fin heat sink, because fine meshing and a high degree of confidence cannot be easily gotten from simulating this profile using commercial CFD tools.

Borrajo-pérez and Reyes-fernández-de-bulnes, (2016), in their studies of the thermal hydraulic performance of a wavy fin having two row of circular tube concluded that the higher heat transfer performance of the wavy fin when compared to that of a plain fin is accounted for by the oscillating movement of the air through the wavy fin model. He also investigated the pressure drop through the model and found the pressure drop to be increasing with the frontal velocity.

Hossain et.al in (Nikam *et al.*, 2015), studied the effect of variation of minimum height, amplitude and wavelength on flow and heat transfer and observed that increasing amplitude and decreasing channel height results in the flow becoming more unstable and thereby increasing friction factor and heat transfer with varying wavelength having minimal effect. Nicenoet *al.* in (Nikam *et al.*, 2015) numerically performed analysis of two dimensional steady and time dependent fluid flow and heat transfer through periodic wavy and arc shaped channels. They found that the flow remains steady up to a critical Reynolds number and beyond a critical value at which transition to an unsteady regime is observed. Heat transfer rate increases as a result of self-sustained oscillations

Among the geometrical variations, Yazicioglu, (2005) maintains that the most commonly applied fin geometry are the rectangular fin geometry because of their simple shape construction, economic impact and effective cooling performance. The heat transfer from the finished system to the external ambient atmosphere according to the researcher may be

obtained by using the convection and radiation heat transfer mechanisms, but the effect of radiation contribution in the total heat transfer rate is quite low due to low value of emissivity of the used fin materials, such as duralumin and aluminum alloys.

Lu *et al.*, (2009) notes that the designer of these fins otherwise called extended surface must optimize the size and spacing of the fin array otherwise using fins can bring more disadvantage than its advantage to the design. Since the attachment of fins increases the surface area but as well lead to increase resistance to air flow, the heat transfer coefficient that is based on the base area of the fin arrays may be less than that of the base plate and if this be the case, we are likely going to have a decrease in the heat transfer coefficient. The convective heat transfer rate between surface and adjacent flow is expressed using the expression of Newton's law of cooling.

$$Q = hA (t_s - t_f) \text{ (Incropera } et al., 2007).$$

And 'h' is a function of the condition within the boundary layer, and is influenced by the surface geometry, the nature of the fluid motion, as well as an assortment of fluid thermodynamic and transport properties.

t_s = surface temperature

t_f = fluid temperature

(Incropera *et al.*, 2007)

(Senthilet *al.* 2017) are of the opinion that heat transfer coefficient is greater with forced circulation of fluid when compared with natural or free convection with optimum fins.

They added that mass flow rates/velocities are important parameters to watch out for while deciding the optimum number of fins when compared to fin materials.

Bilir and Ilken, (2005), Conducted a study on the influence of the changes in fin geometry on heat transfer and pressure drop of a plate fin and tube heat exchanger and observed that the distance between fins has notable effects on pressure drop and that increasing the eccentricity of the fin increases the heat transfer but results in an important reduction in pressure drop. Greater heat transfer and pressure drop results in increased fin height due to increase in heat transfer surface area.

The performance of finned-tube heat exchangers was experimentally investigated with a variation of heat exchanger geometries. The Colburn j-factor decreases with an increase of tube row, and the fin pitch shows negligible influence on the heat transfer performance at large fin pitches. The wavy shape discrete fin can improve the heat transfer performance by approximately 13% (Kim *et al.*, 2004).

2.4. Analytic Solution Of Extend Surfaces

The analytic solution of a uniform cross sectional area fin is contained in many literatures but the same assumptions are made of infinitely long fins (in other words, the fin tip is at same temperature as the adjacent fluid) (Mathiazhagan and Jayabharathy, 2014).

Further assumptions considered are;

- One dimensional conduction in the x-direction
- Steady state condition
- Constant thermal conductivity

- No heat generation
- Constant and uniform convective heat transfer coefficient over the entire surface.

Based on these assumptions the energy equation and boundary condition can be written as;

$$\left(\frac{d^2 T}{dx^2}\right) - m^2(T_0 - T_\infty) \text{ (Mathiazhagan and Jayabharathy, 2014).} \quad 2.5$$

$$T_{(0)} = T_0 \quad 2.6$$

$$T_{(L \rightarrow \infty)} = T_\infty \quad 2.7$$

$$\text{Where } m = \sqrt{\frac{hP}{KA_c}} \quad 2.8$$

The temperature distribution in the fin is given as;

$$T_{(x)} = T_\infty + (T_0 - T_\infty) \exp(-mx) \quad 2.9$$

The total heat transfer by the fin is given as;

$$Q = \sqrt{hPKA_c}(T_0 - T_\infty) \quad 2.10$$

$$\text{Or } Q = \sqrt{hPKA_c}(\theta) \quad 2.11$$

Where, h is the heat transfer coefficient, P is the perimeter of the fin geometry, K is the thermal heat conductivity of the fin material, and A_c is the cross sectional area of the fin, T_∞ is the temperature of the fluid and T_0 is the base surface temperature.

2.5. Fin Performance

As earlier reviewed, that fins are employed in order to increase the effective surface area.

Therefore in order to assess the fact that fins added to a surface area will increase the rate of

heat transfer from that surface, a performance evaluation is carried out by Evaluating the Fin effectiveness, as well as the fin efficiency.

2.5.1. Fin Effectiveness (ε_f)

Fin effectiveness is defined as the ratio of the fin heat transfer rate to the heat transfer rate that would have existed without the fin (Incropera *et al.*, 2007). Therefore the fin effectiveness is given as;

$$\varepsilon_f = \frac{q_f}{hA_{c,b}(\theta_b)} \quad 2.12$$

Where $A_{c,b}$ is the fin base cross-sectional area, q_f is the fin heat transfer rate and θ_b is the temperature at the base of the fin. According to Incropera *et al.*, (2007), in any rational design the value of ε_f must be as large as possible. And that the use of fin can only be justified if the effectiveness value is equal to or greater than two, ($\varepsilon_f \geq 2$).

It can therefore be concluded that the fin effectiveness is influence and aided by the choice of material, basically of high thermal conductivity (such as Aluminum alloy and copper). Increasing the ratio of the perimeter to the cross-sectional area can as well enhance fin effectiveness.

Fin effectiveness can also be quantified in terms of thermal resistance. Where fin resistance may be expressed as;

$$R_t = \frac{\theta_b}{q_f} \quad 2.13$$

$$\varepsilon_f = \frac{R_{t,b}}{R_{t,f}} \quad 2.14$$

(Incropera *et al.*, 2007).

Where, $R_{t,f}$ is the thermal resistance of the fin, and $R_{t,b}$ is the thermal resistance of the base.

2.5.2 Fin Efficiency (η_f)

Fin efficiency is another measure of thermal performance of fin. Fin efficiency therefore is defined as the ratio of the actual heat transfer through the fin to the heat transfer that would occur if the entire fin were at the base temperature.

Therefore,

$$\eta_f = \frac{Q}{hA_f(T_{base} - T_{fluid})} \quad 2.15$$

(Long and Sayma, 2009)

2.5.3. Overall Surface Efficiency (η_o)

Since the fin efficiency evaluates the performance of a single fin, the overall surface efficiency characterizes an array of fins and the base surface to which they are attached.

We therefore have that;

$$\eta_o = \frac{q_t}{h\theta_b A_f} \quad 2.16$$

(Incropera *et al.*, 2007)

q_t , is the total heat transfer from the entire fin array.

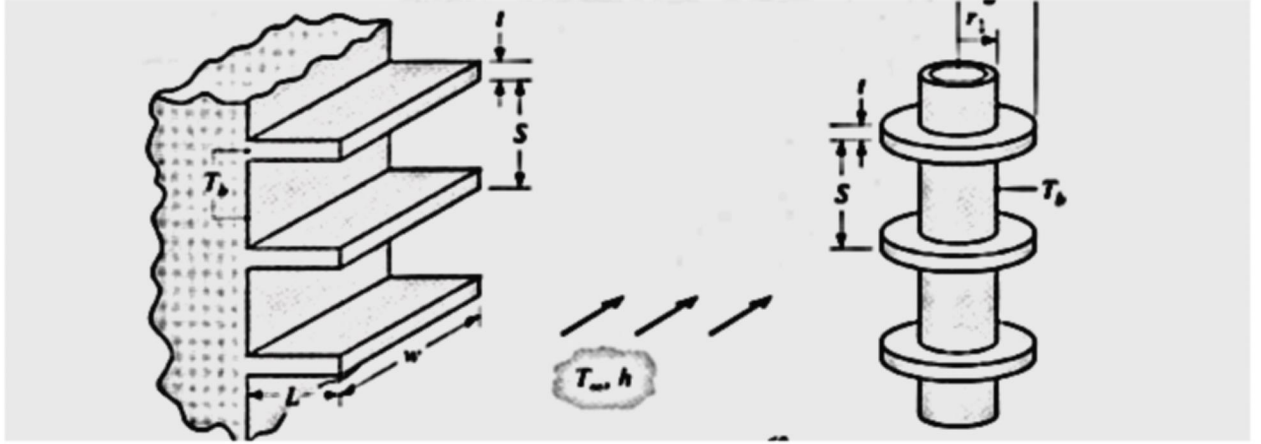


Figure 2.7: Overall performance of fin array (Incropera *et al.*, 2007)

The total rate of heat transfer from fins and the unfinned surface by convection is given as;

$$q_t = N\eta_f h A_b \theta_b + h A_b \theta_b \quad 2.17$$

But though convection coefficient h is assumed to be the same for surfaces attached with fins, and N is the number of fin, η_f is the efficiency of a single fin, A_b is the base area of the fin array and θ_b is the base temperature.

Therefore,

$$q_t = h A_t \left[1 - \frac{N A_f}{A_t} (1 - \eta_f) \right] \theta_b \quad 2.18$$

But substituting equation 2.11 into 1.14 we obtain the overall efficiency as;

$$\eta_o = \left[1 - \frac{N A_f}{A_t} (1 - \eta_f) \right] \quad 2.19$$

(Incropera *et al.*, 2007)

Where, A_f represents the area of a single fin.

CHAPTER 3

3.1. Material and Configuration Geometries

The geometry of the fin array model considered in this study is shown in Figure 3.1 and Figure 3.2. The specifications of the fin array was adopted from a literature review by (Yazicioğlu, 2005) and is shown in the Table 3.1. The material considered for the fin analysis is Aluminum metal due to its high thermal conductivity (about 220W/mK at 300K), low emissivity (0.2 at 297K), high structural strength, durability and light weight. In the case of aluminum fins, the heat transfer is mainly due to the natural convection because the effect of radiation to the total heat transfer is low as a result of low emissivity of aluminum (Bhambare *et al.*, 2016). Air was chosen as the fluid in the flow analysis with atmospheric pressure and temperature at 101325Pa and 306K. The fin array base length, width, height and fin thickness in all configurations were maintained at 95 mm, 110 mm, 5mm and 3 mm, respectively.

The fin samples were modeled using the Solidworks Version 2018 application software. The above fin heights were chosen bearing in mind the extended surfaces in various power transformers. The height of fin ranges from 15 mm to 35 mm, and the fin spacing ranges from 7.3 mm to 22.6 mm. The base area of is 110 mm x 95 mm x 5mm. The fins are modeled to be integral with the base plate and therefore no film is considered. Figure 3.2 shows the wavy fin array geometry.

Table 3.1: Dimension of Fin configuration

| Length of fin L (mm) = 95 | | | | |
|--|---------------------------------|--------------------------------|--------------------------------|--------------------------------|
| Fin wavelength λ(mm) | Fin base Width W(mm) | Fin thickness t(mm) | Base thickness (mm) | Fin amplitude A(mm) |
| 7,10 | 110 | 3 | 5 | 3 |
| SN | Fin Height H(mm) | Fin Spacing S(mm) | Number of fin, n | 3 |
| 1 | 35 | 22.6 | 5 | 3 |
| 2 | 35 | 14.2 | 7 | 3 |
| 3 | 35 | 9.9 | 9 | 3 |
| 4 | 35 | 7.3 | 11 | 3 |
| 5 | 25 | 22.6 | 5 | 3 |
| 6 | 25 | 14.2 | 7 | 3 |
| 7 | 25 | 9.9 | 9 | 3 |
| 8 | 25 | 7.3 | 11 | 3 |
| 9 | 15 | 22.6 | 5 | 3 |
| 10 | 15 | 14.2 | 7 | 3 |
| 11 | 15 | 9.9 | 9 | 3 |
| 12 | 15 | 7.3 | 11 | 3 |

Also in comparing the heat transfer rate between a given straight lengths of wavy fin array with that of a straight uniform cross section fin of the stretched length of the wavy fin array, a separate fin array was modeled to protrude horizontally from a rectangular base and not a protruding vertically from the base. See the added geometrical configuration table and model in Table 3.2.

Table 3.2: Dimension of Compared fin configuration of wavy, stretched, straight fin array

| Fin shape | Wavy fin array | Straight fin array | Stretched wavy fin array |
|---------------------|-----------------------|---------------------------|---------------------------------|
| Parameters | | | |
| base Length, L(mm) | 95 | 95 | 95 |
| Base width, W (mm) | 110 | 110 | 110 |
| Fin height, H(mm) | 35 | 35 | 50 |
| Fin spacing, S (mm) | 22.6 | 22.6 | 22.6 |
| Base thickness | 5 | 5 | 5 |
| Fin thickness | 3 | 3 | 3 |
| Number of fins, n | 7 | 7 | 7 |

The entire wavy fin configurations modeled in solidworks are all shown in Appendix B, both that of the fin configurations used for validation of this research work. Also in Appendix A is shown the working drawing of just one of the wavy fin configuration, that is the configuration of $H = 35$ mm, $S = 14.2$ mm and $\lambda = 7$ mm.

The assumptions made in this study are;

- Convection heat transfer is in three dimension
- The analysis is a steady state analysis
- Radiation heat transfer is neglected
- Constant and uniform convective heat transfer coefficient over the entire surface

- There is no heat generation

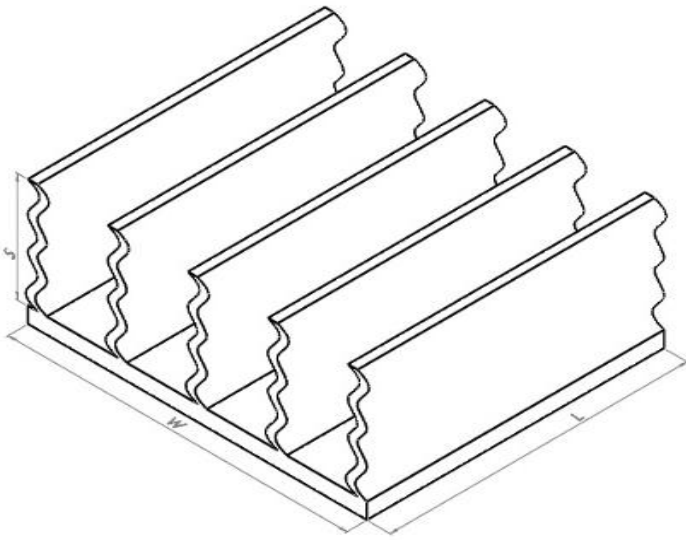
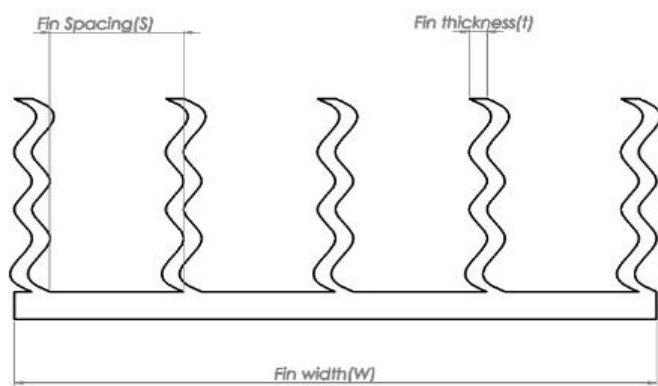
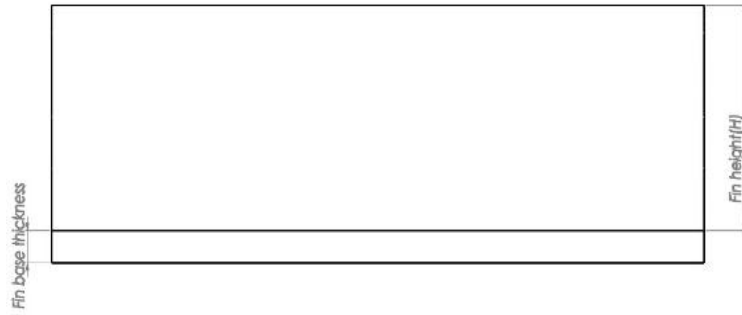


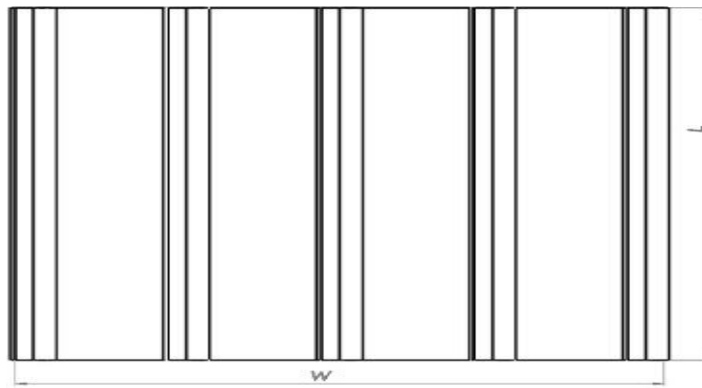
Figure 3.1: Wavy fin configuration geometry



a. Front view



b. Side view



c. Top or plan view

Figure 3.2: Wavy fin configuration geometry views.

3.2. Theoretical Analysis of heat transfer rate

The theoretical analysis of the wavy fin was based on the number of assumptions as seen in section 2.4 of this work. The deviation is in the shape of the fin. In the analysis shown in section 2.4, a uniform cross sectional rectangular straight fin was used but this study is particular about the wavy fin geometry.

The wavy fin is usually considered to be a sinusoidal wave so as to determine the effective flow length, which also enhances the surface area.

Referring to the Figure 3.1a and 3.1b, the length of a wavy fin is given as;

$$F(x) = A \sin(2\pi x/\lambda) \quad 3.1$$

$$Le = 2 \int_0^{\lambda/2} \sqrt{1 + [f'(x)]^2} dx \quad 3.2$$

(Nikam *et al.*, 2015)

Handbook approximations as well as mathematical software can be used to determine the elliptic integral. With the effective flow length, Le determined, the effective flow area can be determined of the wavy fin and used to theoretically determine the heat transfer in the wavy fin array.

3.3. Mathematical Theories/Governing Equations

Numerical analysis of heat transfer in finis based on finite volume method as used by Solidworks flow simulation solver. The simulations are conducted in accordance with the sets of partial differential equations defined under Reynolds averaged Navier-Stoke Model(Pati *et al.*,2018). The governing equations such as continuity, momentum and energy equations for 3-D Cartesian coordinates are shown below in vector notations.

1. Continuity Equation

$$\frac{\partial \rho}{\partial t} + \nabla \cdot (\rho \vec{V}) = 0 \quad 3.3$$

2. Momentum equation

$$\rho \frac{Du}{Dt} = -\frac{\partial P}{\partial x} + \nabla \cdot (\mu \nabla u) \quad 3.4a$$

$$\rho \frac{Dv}{Dt} = -\frac{\partial P}{\partial y} + \nabla \cdot (\mu \nabla v) \quad 3.4b$$

$$\rho \frac{Dw}{Dt} = -\frac{\partial P}{\partial z} + \nabla \cdot (\mu \nabla w) \quad 3.4c$$

3. Energy equation

$$\rho \frac{Di}{Dt} = \nabla \cdot (K \nabla T) - \rho \nabla \cdot (V) + \emptyset \quad 3.5$$

3.4 Simulation Procedures

The simulation was carried out using Solidworks flow simulation in Solidworks version 2018. And in carrying out the thermal heat transfer numerically in fin array the following procedures were followed as highlighted and discussed as follow:

- Geometrical Modeling of the Fin
- Determining the computational domain
- Selection of Materials
- Selection and application of boundary conditions
- Meshing of the solid geometry and the fluid domain and
- Results

3.4.1 Geometrical Modeling of the Fin Array

The modeling was done on the 2-D sketch interface in Solidworks by first selecting the Unit system (millimeter, gram and second), choosing the sketch plane (top plane). Thereafter a rectangular too was chosen to generate the base and then a line tool was used to generate the fins as well as a smart dimension too selected to dimension the 2-D object to given dimensions, as well as a trim too selected to trim off unwanted lines. The 2-D object is then extruded using the extruded boss/base tool from the feature tool tray to obtain the fin array geometries.

3.4.2 Determining the computational domain

The computational domain is automatically created by the Solidworks flow simulation for the fluid surrounding. It can only be adjusted to ones preferred dimensions by right clicking on it and clicking on edit computational domain.

3.4.3 Material Selection

Before running the simulation the materials from the material catalogue was selected and applied and to the solid (fin array). In this work the materials selected and applied is Aluminum metal owing to its high thermal conductivity and high strength and durability.

3.4.4 Selection of Boundary Conditions

The boundary conditions were chosen such that; the fin and base plate was assigned as solid domain. The enclosure (that is the computational domain) automatically becomes the fluid domain. The base plate back surface was taken as real wall 1, with temperature value assigned to it as shown in Table 3.3. The remaining surfaces of the fin array or assembly were taken as real wall 2 with a convective heat transfer coefficient and air duct temperature assigned to it as shown in Table 3.3. Solidworks flow simulation automatically assigns the inlet and outlet pressure, the surrounding fin temperature and the adiabatic condition to the walls of the computational domain.

Table 3.3:Simulation and Boundary Parameters

| Fluid | Air |
|---|-----------------------|
| Fluid or Ambient temperature, $T_a(^{\circ}\text{C})$ | 27 |
| Atmospheric pressure (Pa) | 101325 |
| Boundary Condition | Real wall |
| Wall temperature, $T_w(^{\circ}\text{C})$ | 45, 60, 90, 120, 150 |
| Heat transfer coefficient, $h(\text{W}/\text{m}^2\text{k})$ | 20 |
| Material applied | Aluminum metal |
| Analysis type | External |
| Flow Characteristics | Turbulent and laminar |

3.4.5 Meshing of the Fin array Solid

The meshing was done by right clicking on the mesh tool and selecting, create mesh. Standard meshing without mesh refinement was done. Also, an automatic meshing with mesh level 4 of 7 and minimum mesh gap size of 3mm was used.

3.4.6 Results

In Solidworks the goals of the simulation analysis is first chosen before the meshing and running of the analysis. Once the calculations (or iterations are done) the results of the selected goals are then loaded in the result section for extraction and analysis

3.5 Validation of simulation Result

In other to check if the results obtained by simulation in this study were valid and reliable, experimental results data from(Yardi *et al.*, 2017) in his experimental study of “optimization of fin spacing by analyzing the heat transfer through rectangular fin array configuration by natural convection”, as well as the configuration geometry of the fin array. This fin array geometry was modeled using Solidworks and then simulated with solidworks flow simulation and the results compared to the experimental results. See the configuration geometry table in Table 3.4.

Table 3.4:Fin array Configuration geometry

| No. of Fin (n) | Height H(mm) | Length of fin L (mm) | Width of fin W (mm) | Thickness of fin T (mm) | Fin spacing S (mm) | Base thickness (mm) |
|----------------|--------------|----------------------|---------------------|-------------------------|--------------------|---------------------|
| 4 | 15 | 95 | 110 | 2 | 28 | 5 |
| 5 | 15 | 95 | 110 | 2 | d20.5 | 5 |
| 6 | 15 | 95 | 110 | 2 | 16 | 5 |
| 8 | 15 | 95 | 110 | 2 | 10.85 | 5 |

CHAPTER FOUR

4.0 RESULTS AND DISCUSION

4.1. Introduction

The simulation data obtained from thirty four (34) different fin configurations as well as the surface plots are presented and discussed here in this chapter. These results are used to reveal the contribution of geometric parameter such as fin spacing, fin height and fin shape, as well as the effects of base-to-ambient temperature variation on the steady state heat transfer rates from fin surfaces. The simulation data are presented also in several figures to analyze the effect of each parameter separately.

The convection heat transfer rates from wavy fin arrays projecting from a horizontal rectangular base are drawn against the base-to-ambient temperature difference for fin spacing $S = 7.3\text{mm}$, $S = 9.9\text{mm}$, $S = 14.2\text{ mm}$, and $S = 22.6\text{mm}$ and wavelength $\lambda = 7\text{ mm}$ and $\lambda = 10\text{mm}$ all of the same fin length, $L = 95\text{mm}$ respectively. In addition, the convective heat transfer rate was also plotted against the base to ambient temperature difference for wavy fin shape array and its equivalent stretched length of rectangular straight fin array, of the same fin spacing. Each Figure presents the results plotted for three fin heights $H = 15\text{ mm}$, $H = 25\text{ mm}$ and $H = 35\text{ mm}$ at each wavelength.

4.2 Results and Analysis

A summary of the simulation results are also presented in tabular forms as shown in Table 1 of appendix A. The mesh pattern, the surface plot for the at least one sample of the fin

configuration model of the wavy fin is also displayed in Figure 4.1. The surface plot shows the temperature distribution along the fin surface from the base to the top of the fin. It also reveals that the temperature reduces from the base towards the fin tip. See Figure 4.1 through Figure 4.2c.

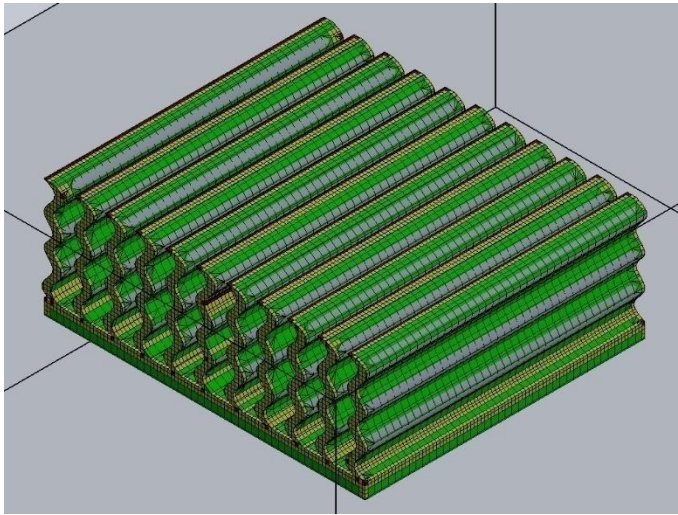


Figure 4.1: Meshing of Fin array

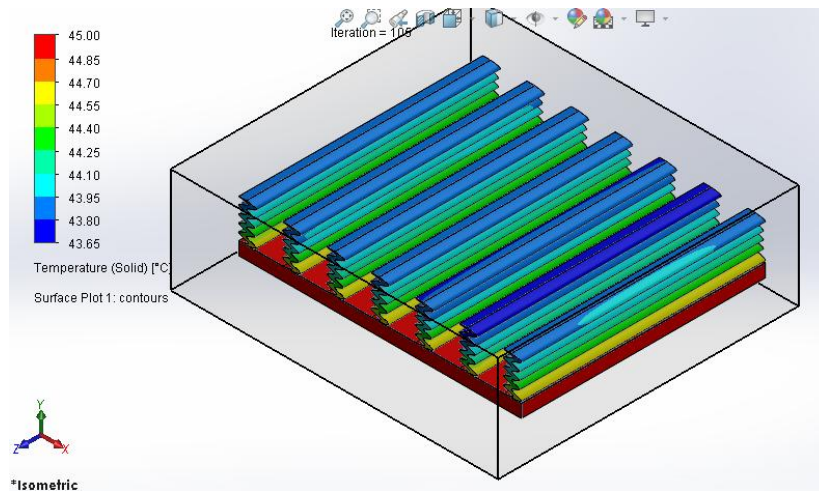


Figure 4.2a: Surface plot showing the solid temperature of wavy fin array of $H = 25$ mm, $s = 9.9$ mm at wall temperature of 45°C

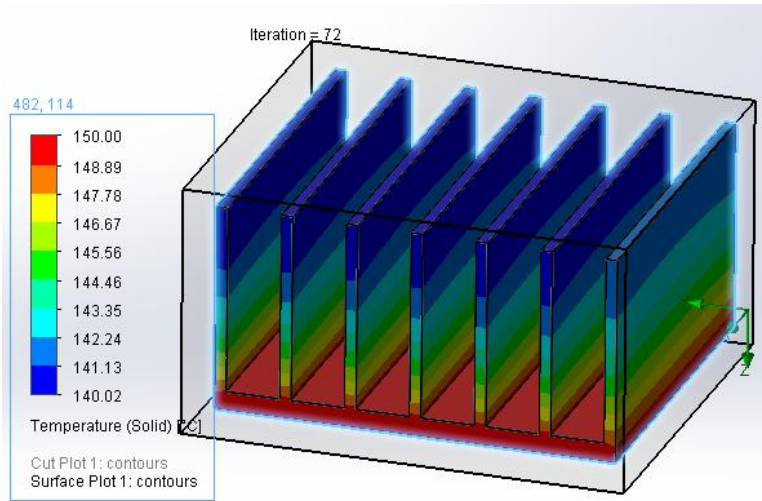


Figure 4.2b: Surface plot showing the solid temperature of rectangular straight fin array geometry at wall temperature of 150°C

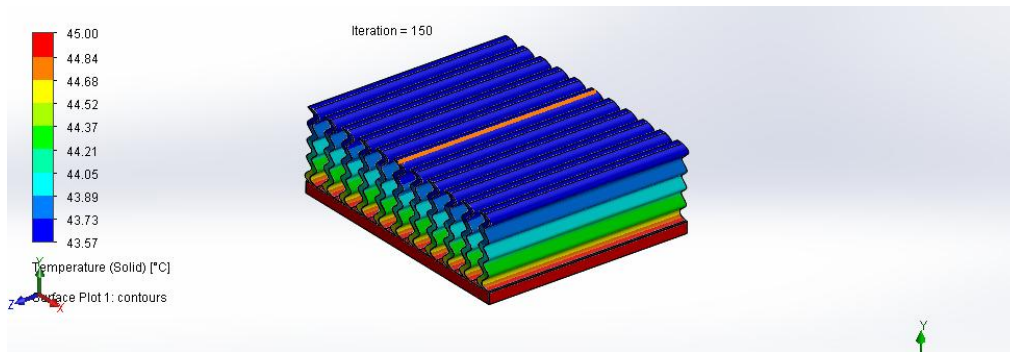
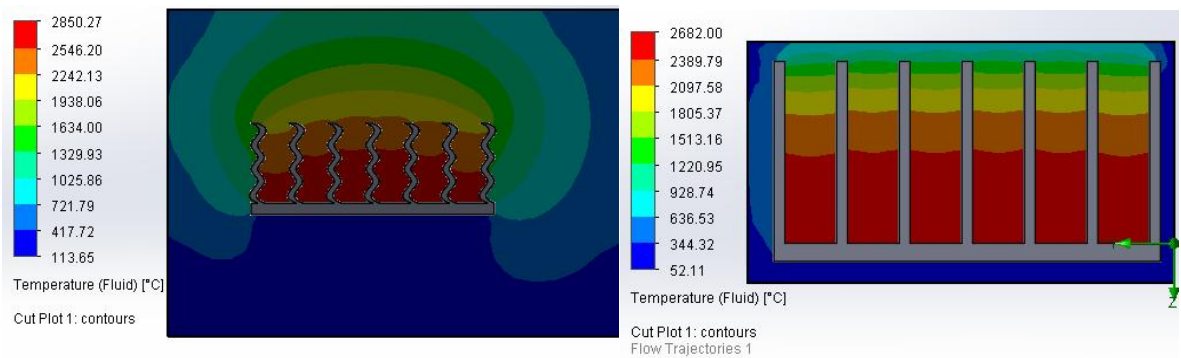


Figure 4.2c: Surface plot showing the solid temperature of wavy fin array of $H = 25$ mm, $S = 7.3$ mm, $\lambda = 7$ mm at wall temperature of 45°C

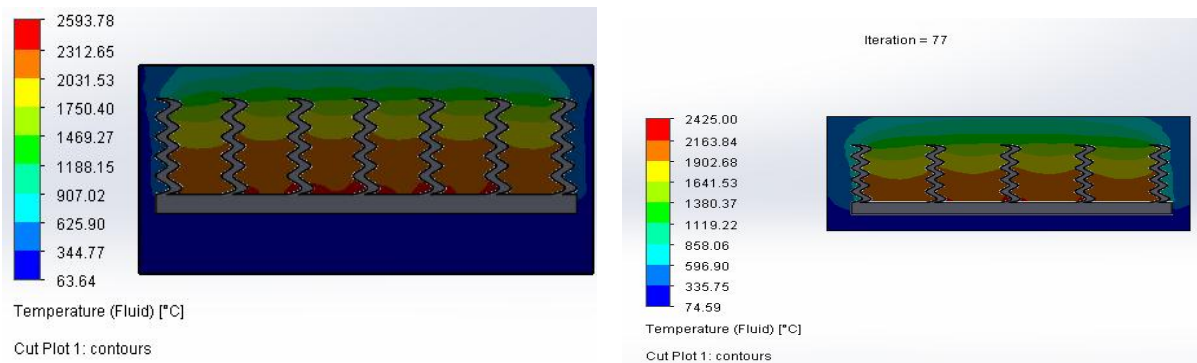
When observed from the validation graph in Figure 4.3 above it was noticed that the experimental graph of the heat transfer rate at 15°C base-to-ambient temperature when compared with that of simulation graph of heat transfer rate at same condition seemed to be so close at the various spacing except for the spacing at 16 mm which gives 7.34% error which was found to be the maximum error obtained, and also within the allowable percentage error range as maintained by (Yardi *et al.*, 2017). With these results obtained it therefore entails that every simulation results data that would be obtained at this numerical

study is therefore valid and trusted. The Cut plots of some of the fin array showing the fluid temperature contour was plotted as displayed in Figure 4.3d. From the cut plot is generally observed that the highest fluid temperature is the closest to the base of the fin and reduces towards the tip of the fin. The lowest temperature observed to be beneath the fin base. This is as a result of the principle of natural convection due to buoyancy force. That is, the heat energy transfer is as a result of density gradient.



(a) $H = 35$ mm, $S = 14.2$ mm at $T_w = 150^\circ\text{C}$

(b) $H = 35$ mm, $S = 14.2$ mm $T_w = 150^\circ\text{C}$



(c) $H = 25$ mm, $S = 14.2$ mm at $T_w = 120^\circ\text{C}$

(d) $H = 25$ mm, $S = 14.2$ mm at $T_w = 120^\circ\text{C}$

Figure 4.3: Cut plot of fluid temperature

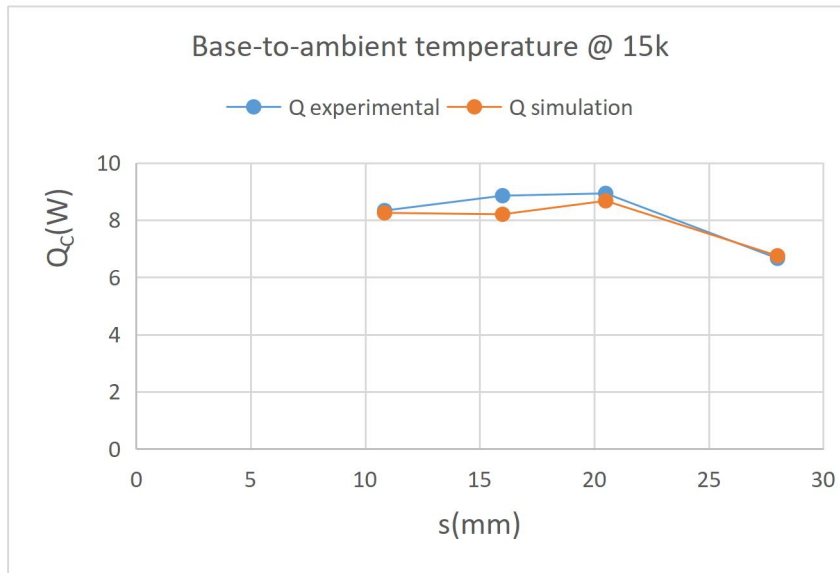


Figure 4.4: Heat Transfer Comparison by experiment and simulation

Table 4.1: Experimental and Simulation Heat transfer rate Result at $\Delta T = 15^\circ\text{C}$

| No. Of fins | Heat transfer (W) | | % Error | Fin temperature ($^\circ\text{C}$) | | % Error |
|-------------|-------------------------|-------------------------|---------|--------------------------------------|-------------------------|---------|
| | Q _{experiment} | Q _{simulation} | | T _{experiment} | Q _{simulation} | |
| 4 | 6.66 | 6.75 | 1.35 | 48.00 | 49.82 | 3.79 |
| 5 | 8.93 | 8.67 | 2.99 | 45.90 | 49.80 | 8.5 |
| 6 | 8.85 | 8.20 | 7.34 | 46.00 | 49.80 | 8.26 |
| 8 | 8.33 | 8.25 | 0.96 | 49.3 | 49.70 | 1.01 |

When the graph in Figures 4.5 through 4.10 are considered together, it can be concluded that at low base to ambient temperature difference inputs, the convection heat transfer rate from the three fins are closer than those at high base-to-ambient temperature difference in consequent of the variations in the fin spacing and the fin height. As observed in all of these six figures, the convection heat transfer rate from fin arrays for the fin spacing values, $S = 7.3 \text{ mm}$ is higher than those of the remaining fin spacing, at any given base-to-ambient temperature difference and fin height.

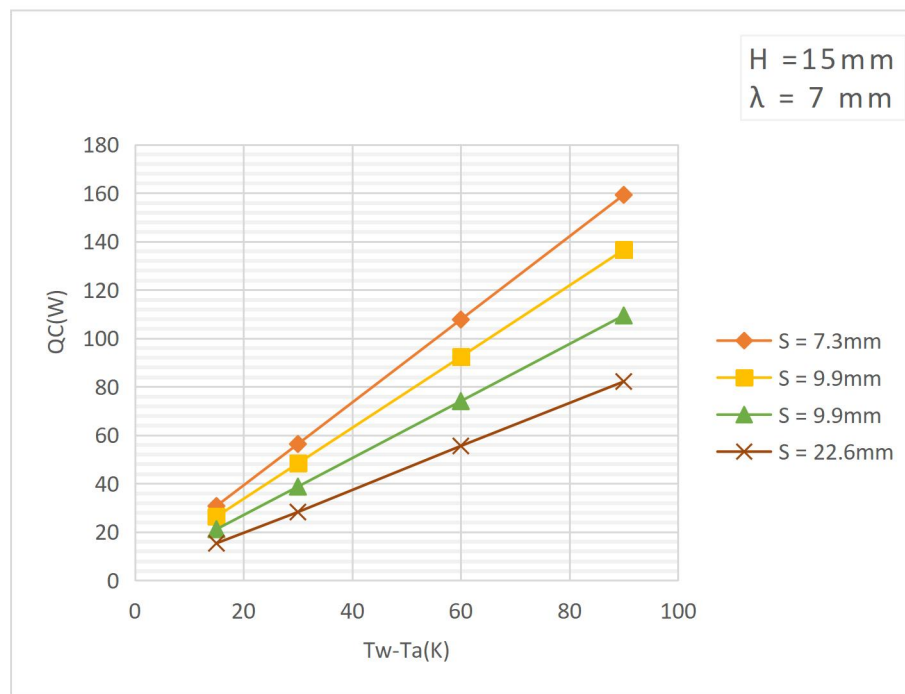


Figure 4.5: Variation of convective heat rate with Fin spacing at $H = 15 \text{ mm}$, $L = 95$ and, $\lambda = 7 \text{ mm}$

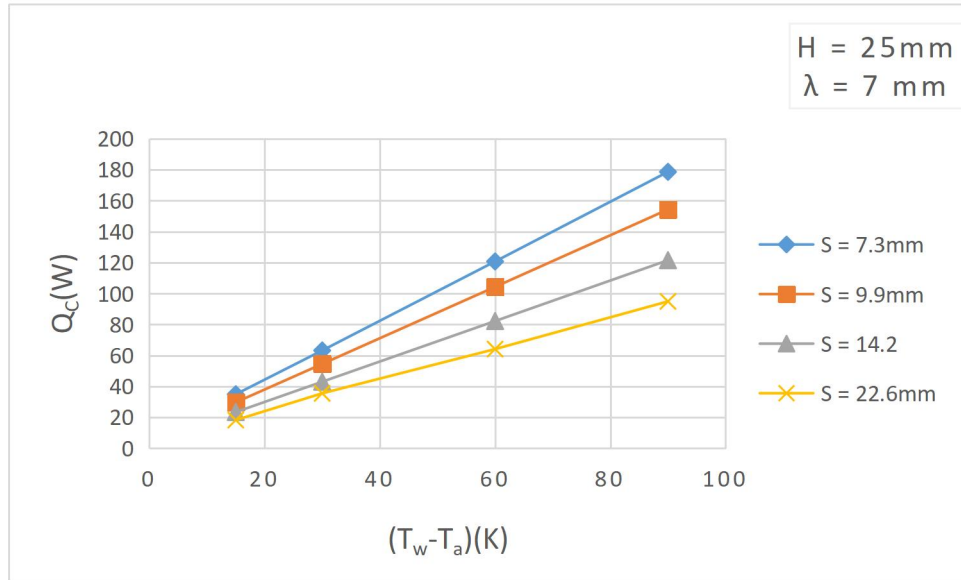


Figure 4.6: Variation of convective heat transfer rate with fin spacing at $H=25$ mm, $L=95$ mm and $\lambda=7$ mm

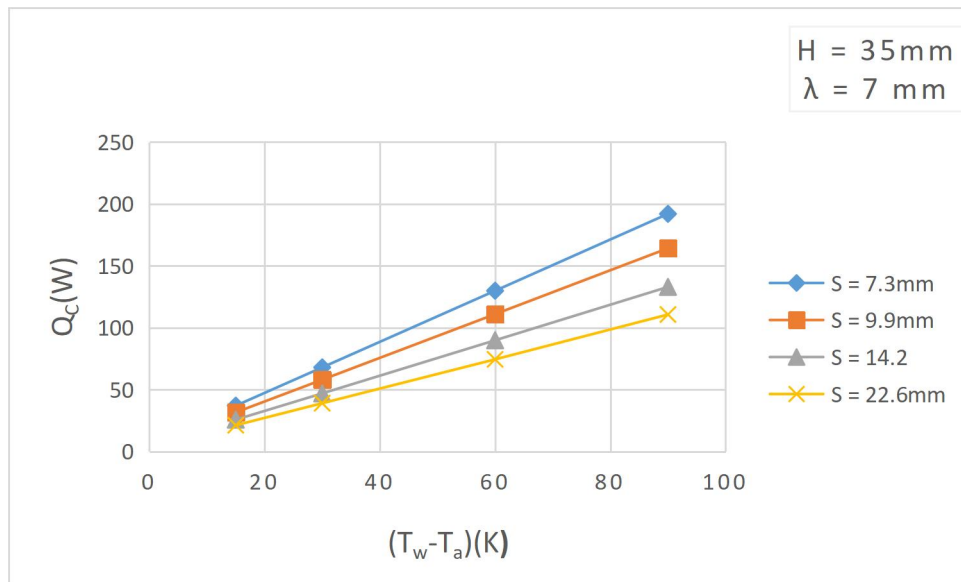


Figure 4.7: Variation of convective heat transfer rate with fin spacing at $H=35$ mm, $L=95$ mm and $\lambda=7$ mm

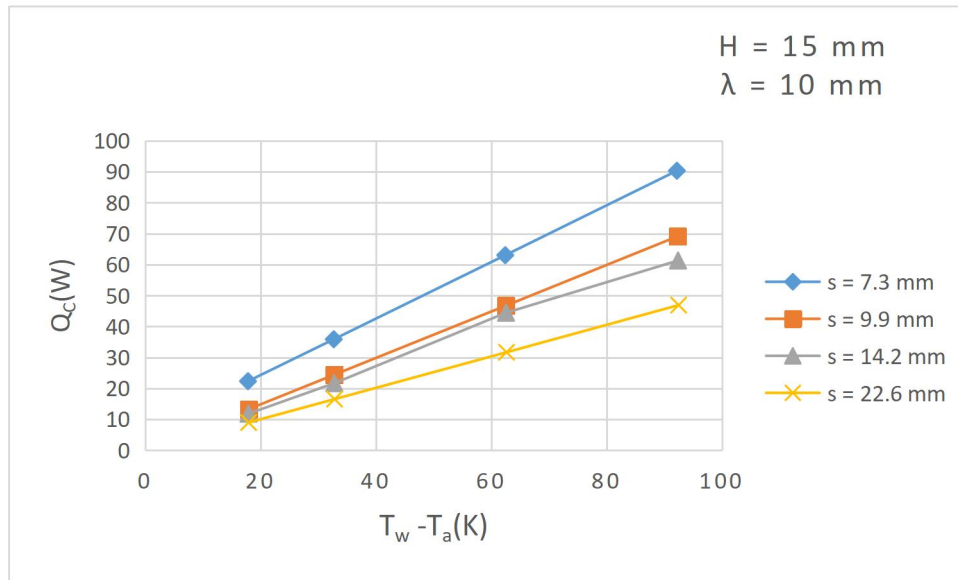


Figure 4.8: Variation of heat transfer rate with fin spacing at $H=15$ mm, $L=95$ mm and $\lambda=10$ mm

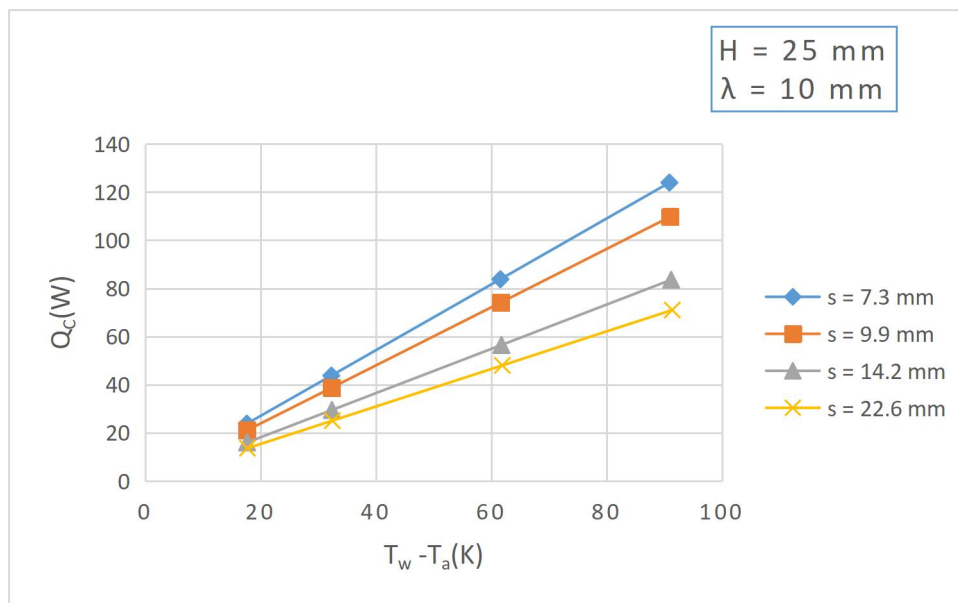


Figure 4.9: Variation of convective heat transfer rate with fin spacing at $H=25$ mm, $L=95$ mm and $\lambda=10$ mm

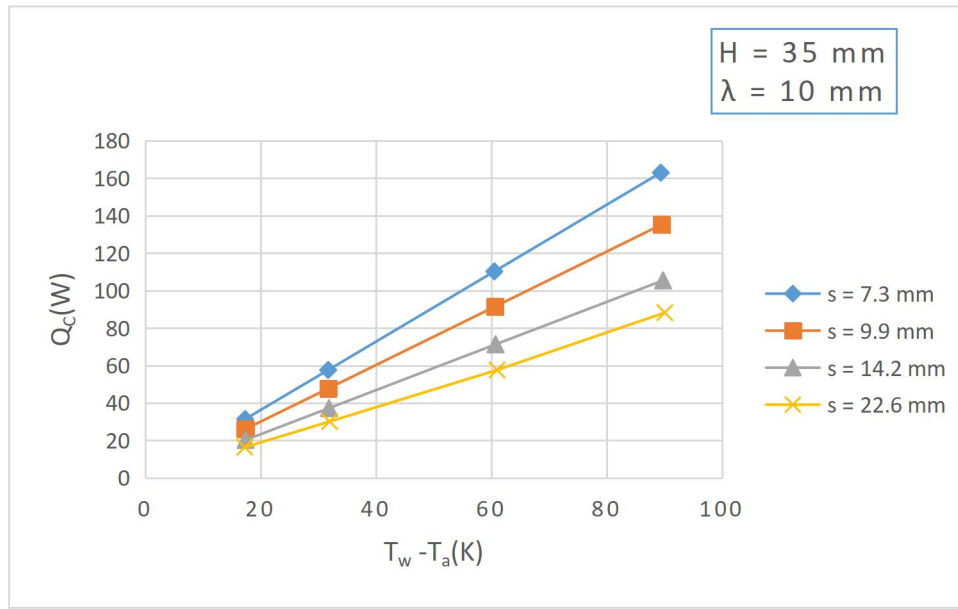


Figure 4.10: Variation of convective heat transfer rate with fin spacing at $H=35$ mm, $L=95$ mm and $\lambda=10$ mm

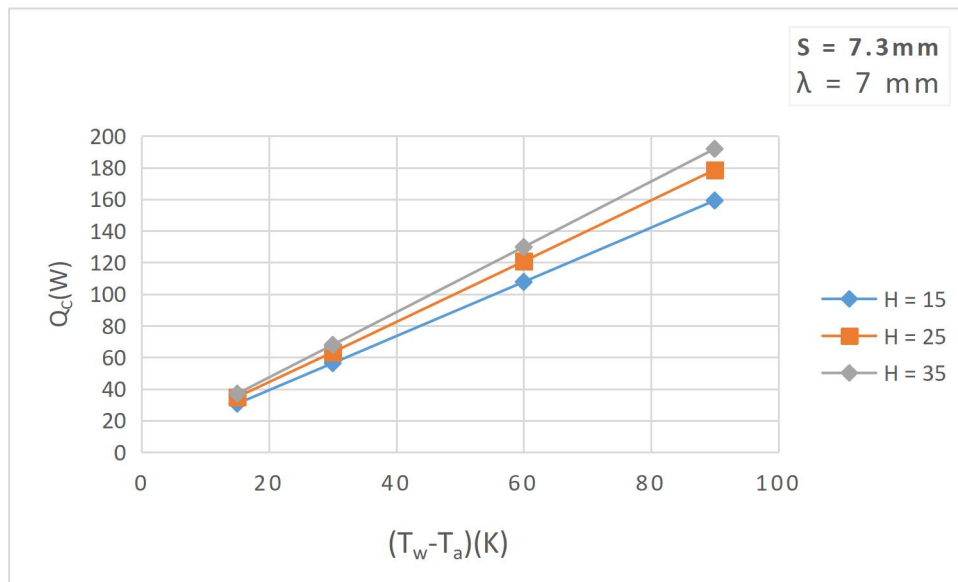


Figure 4.11: Variation of convective heat transfer rate with fin height at $S=7.3$ mm, $L=95$ mm and $\lambda=7$ mm

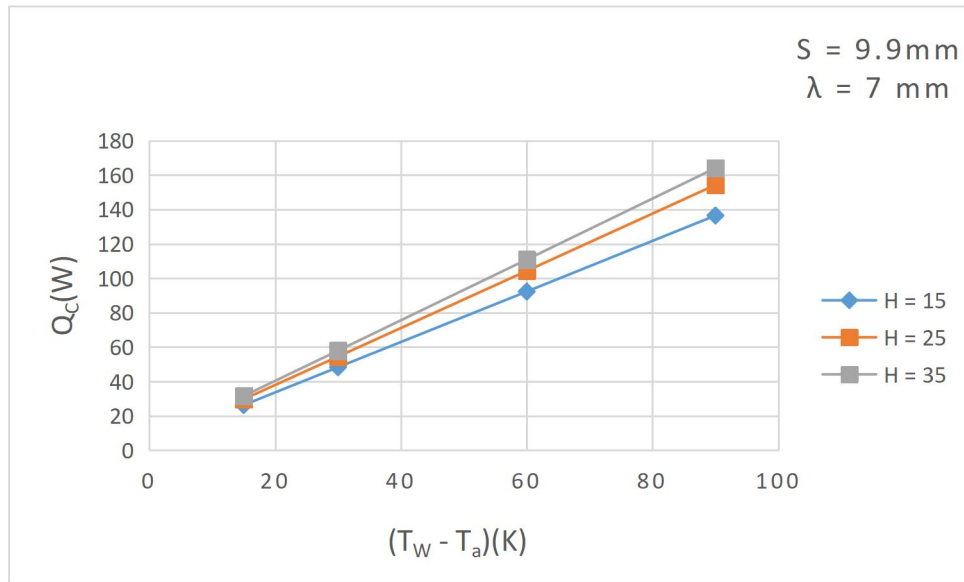


Figure 4.12: Variation of convective heat transfer rate with fin height at $S=9.9 \text{ mm}$, $L=95 \text{ mm}$ and $\lambda=7 \text{ mm}$

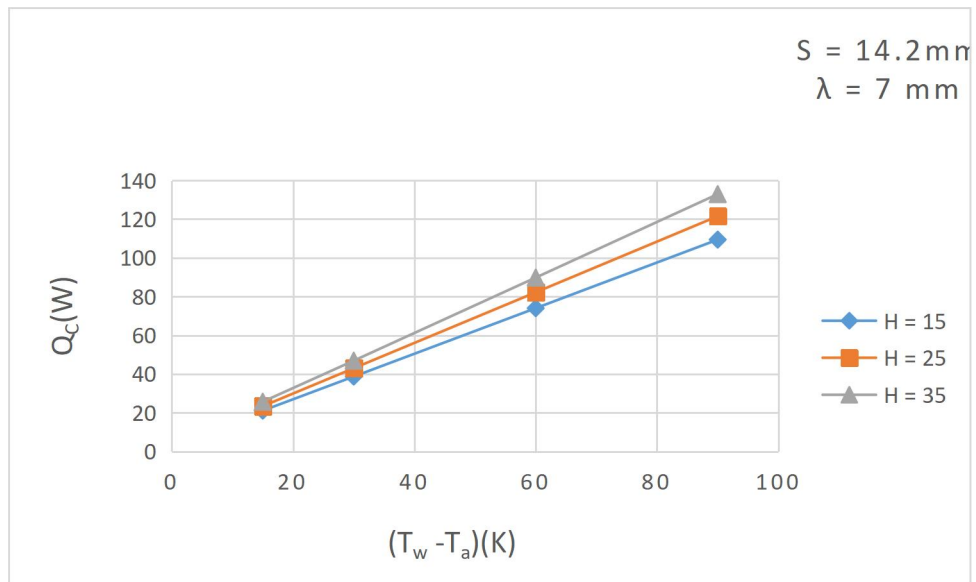


Figure 4.13: Variation of convective heat transfer with fin height at $S=14.2 \text{ mm}$, $L=95 \text{ mm}$ and $\lambda=7 \text{ mm}$

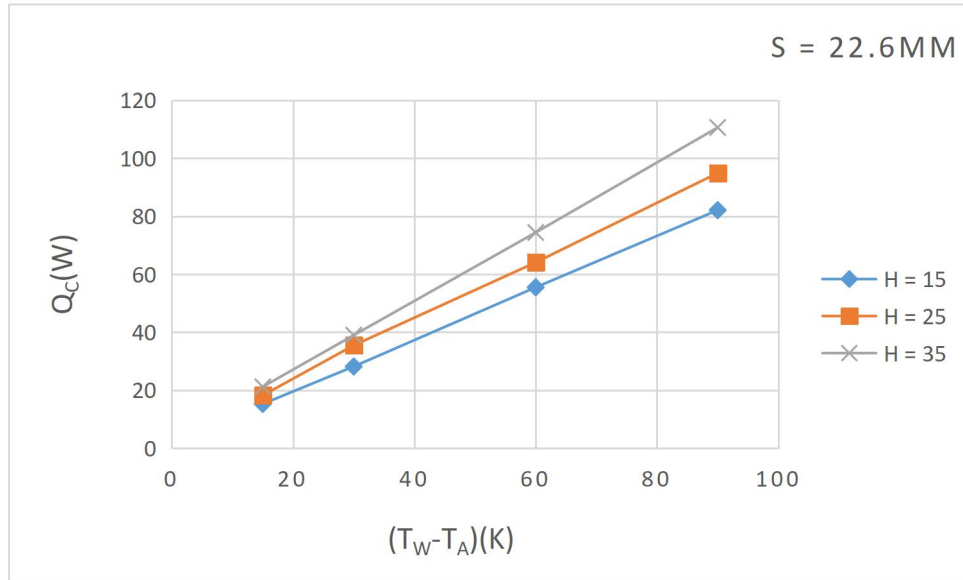


Figure 4.14: Variation of convective heat transfer rate with fin height at $S=14.2\text{mm}$, $L=95\text{mm}$ and $\lambda = 7 \text{ mm}$

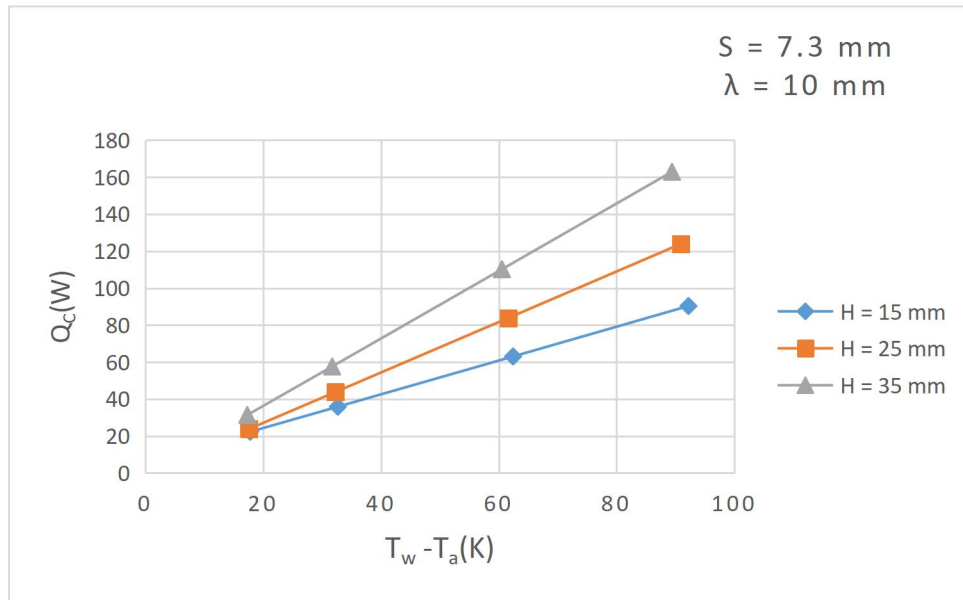


Figure 4.15: Variation of convective heat transfer rate with fin height at of $S=7.3\text{mm}$, $L=95\text{mm}$ and $\lambda = 10 \text{ mm}$

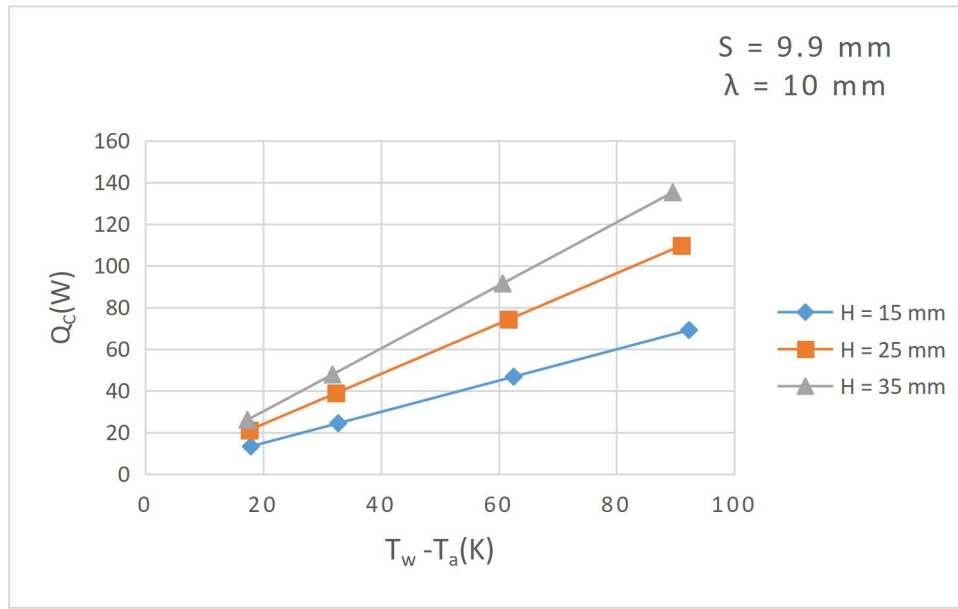


Figure 4.16: Convective heat transfer rate variation with fin height of $S=9.9$ mm, $L=95$ mm and $\lambda = 10$ mm

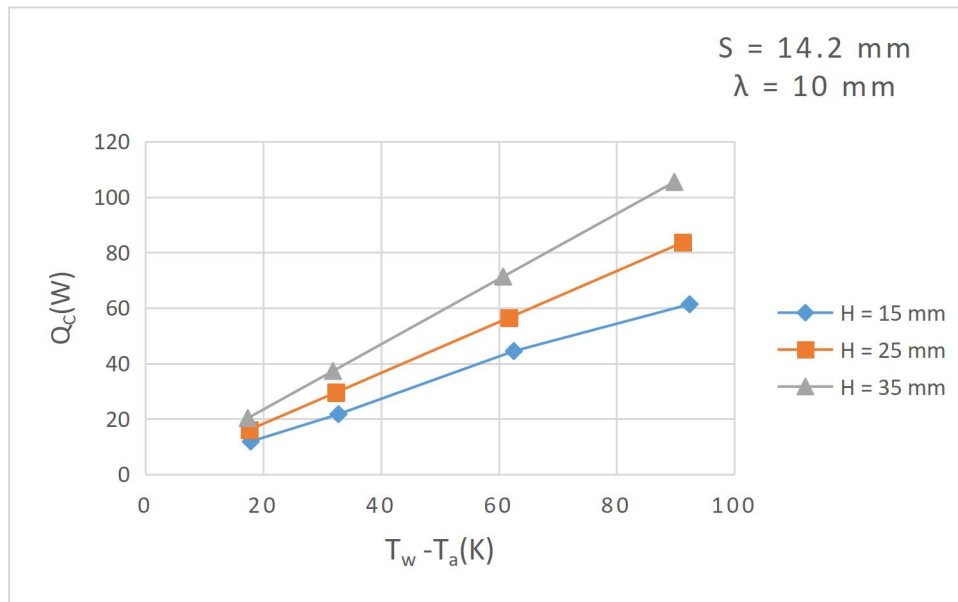


Figure 4.17: Convective heat transfer rate variation with fin height at $S=14.2$ mm, $L=95$ mm and $\lambda = 10$ mm

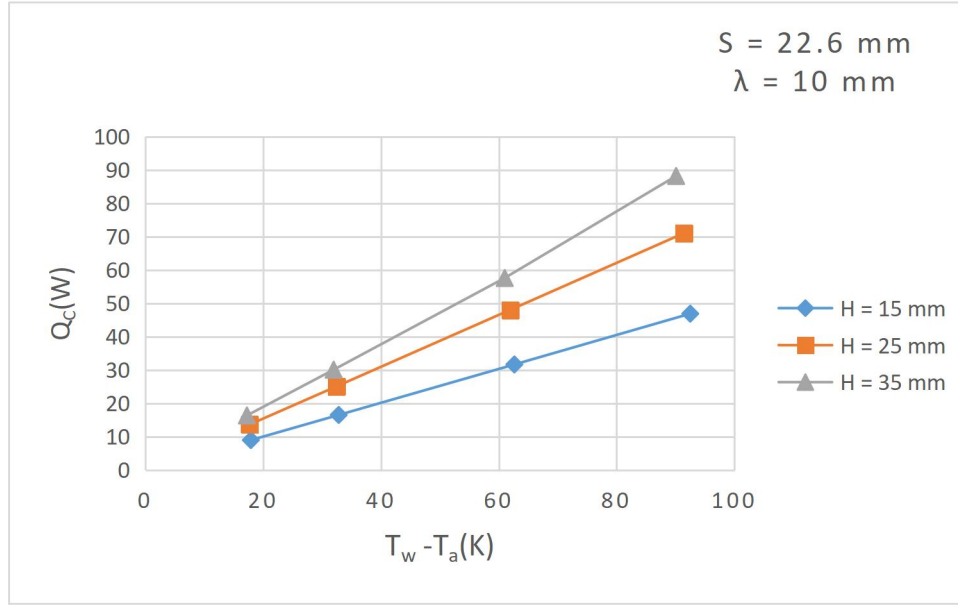


Figure 4.18: Convective heat transfer rate variation with fin height at $S=14.2$ mm, $L=95$ mm and $\lambda = 10$ mm

As observed in Figures 4.11 to 4.16, the convection heat transfer rate from fin arrays depends on fin height, fin length, fin spacing and base-to-ambient temperature difference as well as the fin wavelength. It is noticed that the convective heat transfer rates from the fin arrays increases with increase in the fin height and base-to-ambient temperature difference for the both fin wavelength.

In Figures 4.19 to 4.23, it can be clearly seen what the result of Base-to-ambient temperature difference on convection heat transfer rate is. In these figures, convection heat transfer rates are plotted against fin spacing. The figures are for fin length of $L=95$ mm, heights of $H=15$ mm, $H=25$ mm and $H=35$ mm and wavelengths of $\lambda = 7$ mm, $\lambda = 10$ mm respectively.

From Figures 4.19 to 4.23, it is observed that the convection heat transfer rate from the wavy fin array began to drop as the fin spacing kept increasing at every base-to-ambient temperature difference. This implies that as the fin array spacing increases less number of fins are accommodated in the array. This so much agrees with the findings of Sharafian *et al.*, (2014) on the impact of fin spacing on temperature distribution. In other words, the convection heat transfer rate in the fin array will increase as the fin spacing of the fin array decreases and vice versa. This is due to the fact that as the fin spacing decreases more number of fins are accommodated in the array, thereby increasing the total convective area in the fin array.

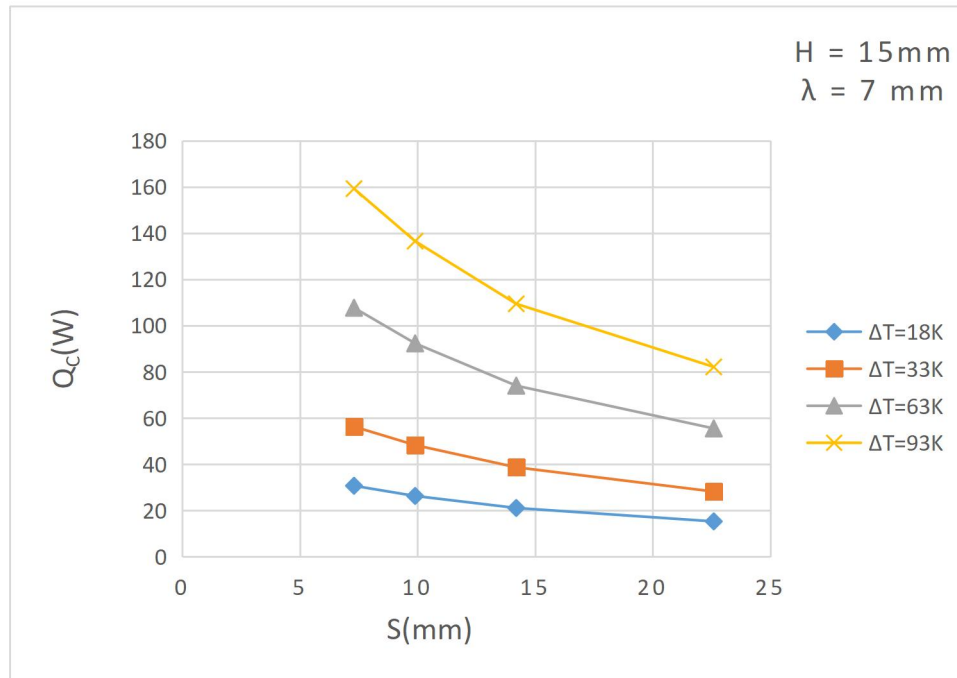


Figure 4.19: Convective heat transfer rate variation with base-to-ambient temperature difference at $H=15 \text{ mm}$, $L=95 \text{ mm}$ and $\lambda = 7 \text{ mm}$

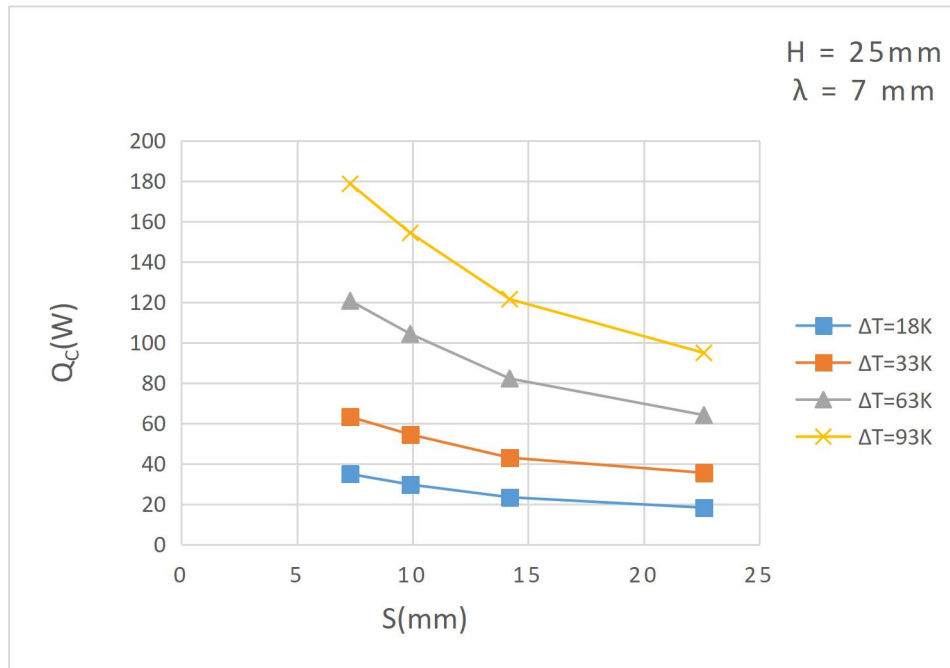


Figure 4.20: Convective heat transfer rate variation with base-to-ambient temperature difference at $H=25$ mm, $L=95$ mm and $\lambda = 7$ mm

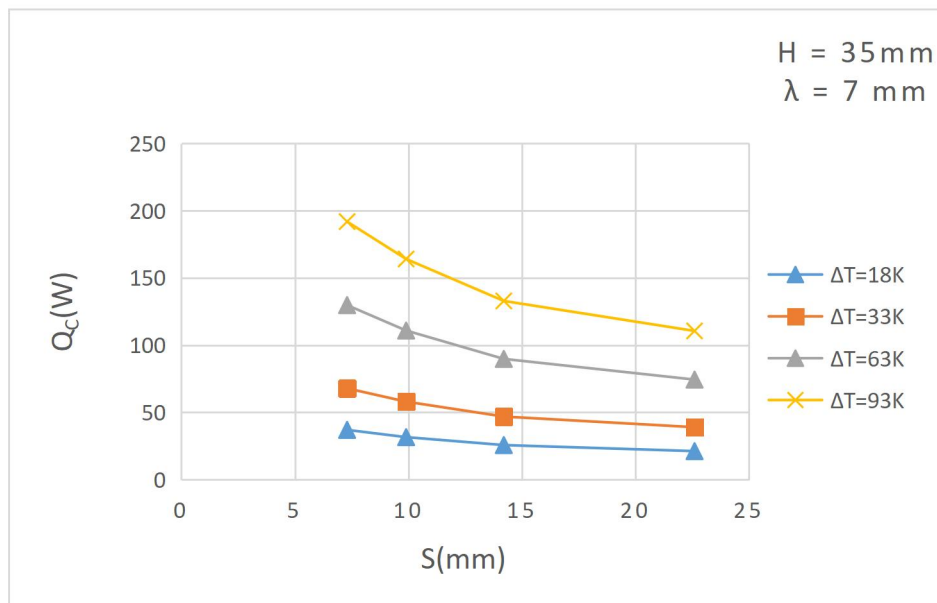


Figure 4.21: Convective heat transfer rate variation with base-to-ambient temperature difference at $H=35$ mm, $L=95$ mm and $\lambda = 7$ mm

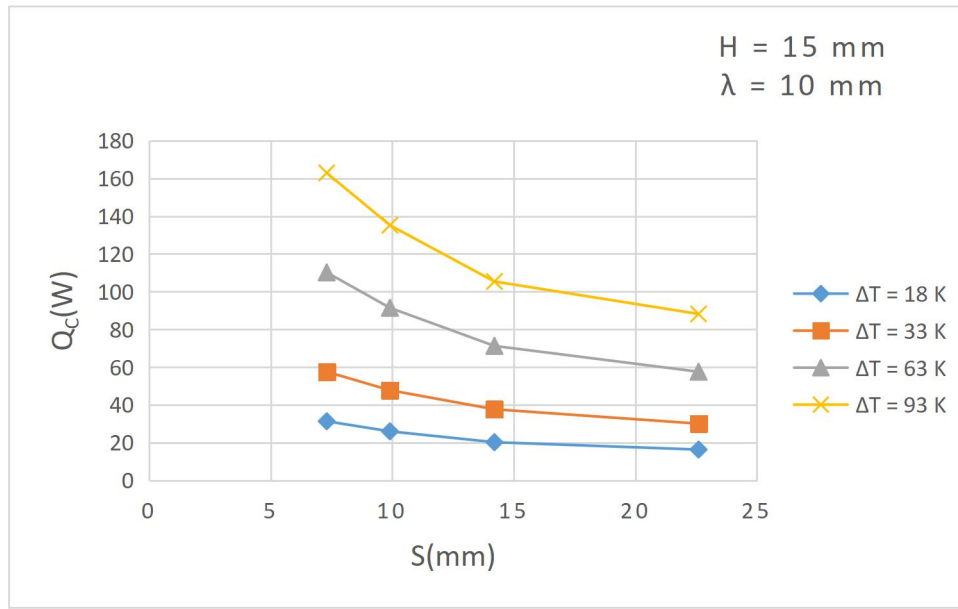


Figure 4.22: Convective heat transfer rate variation with base-to-ambient temperature difference at $H=15$ mm, $L=95$ mm and $\lambda = 10$ mm

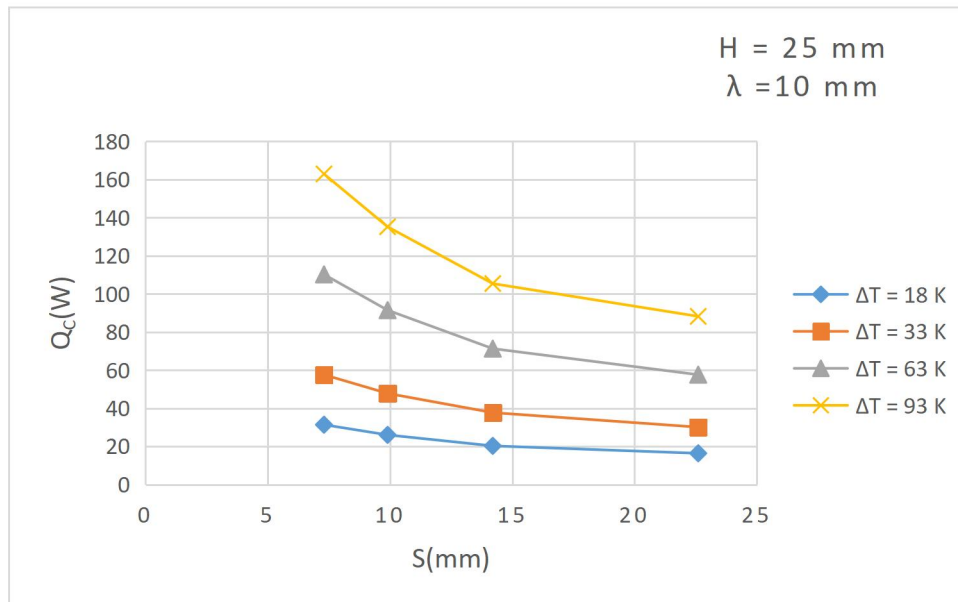


Figure 4.23: Convective heat transfer rate variation with base-to-ambient temperature difference at $H=25$ mm, $L=95$ mm and $\lambda = 10$ mm

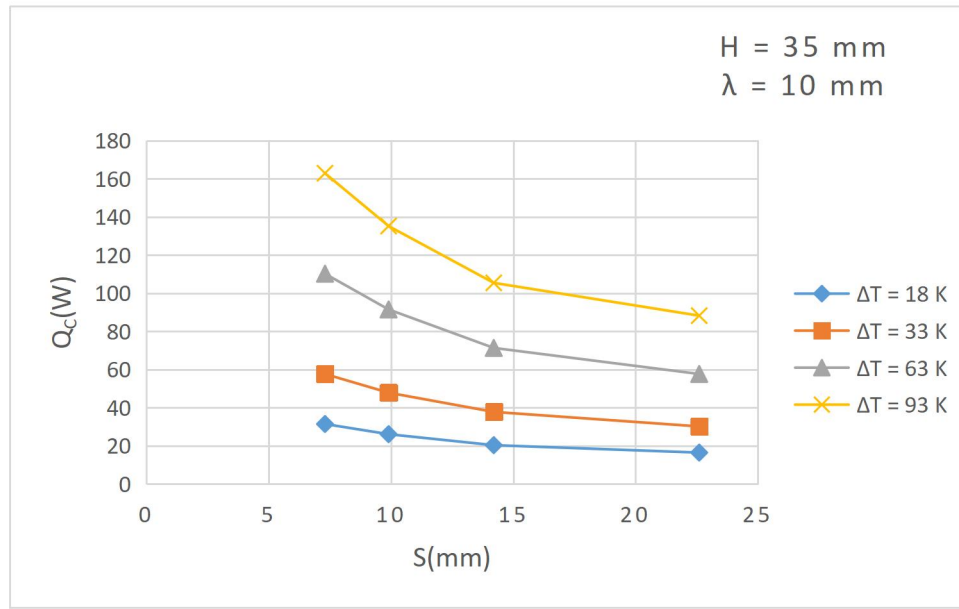


Figure 4.24: Convective heat transfer rate variation with base-to-ambient temperature difference at $H=35$ mm, $L=95$ mm and $\lambda = 10$ mm

It is also observed from the figures plotted above that the height at $H = 35$ mm has the highest rate of convection heat transfer followed by height $H = 25$ mm and then $H = 15$ mm. In other words, the convective heat transfer rate increases with increase in fin height. With this observation it can be concluded that the convective heat transfer rate is also a function of the height of fin, the spacing between fins, and the base-to-ambient. Refer to table 1 in appendix A.

In considering the effect of fin wavelength on the heat transfer rate from Figure 4.5 through Figure 4.20, it is observed that the convective heat transfer rate decrease with increase in the wavelength irrespective of the fin height, length, spacing and base-to-ambient temperature. The heat transfer rate at $\lambda = 7$ mm is higher than $\lambda = 10$ mm irrespective of other parameters considered.

The rate of convective heat transfer with respect to base-to-ambient temperature difference can be seen in Figure 4.25 for a chosen wavy fin array geometry of $H = 35\text{mm}$ and it stretched height into a straight rectangular fin array, as well as a straight rectangular fin array equivalent of the wavy fin array height with all of these trio having same fin separation distance of $S = 14.2\text{mm}$.

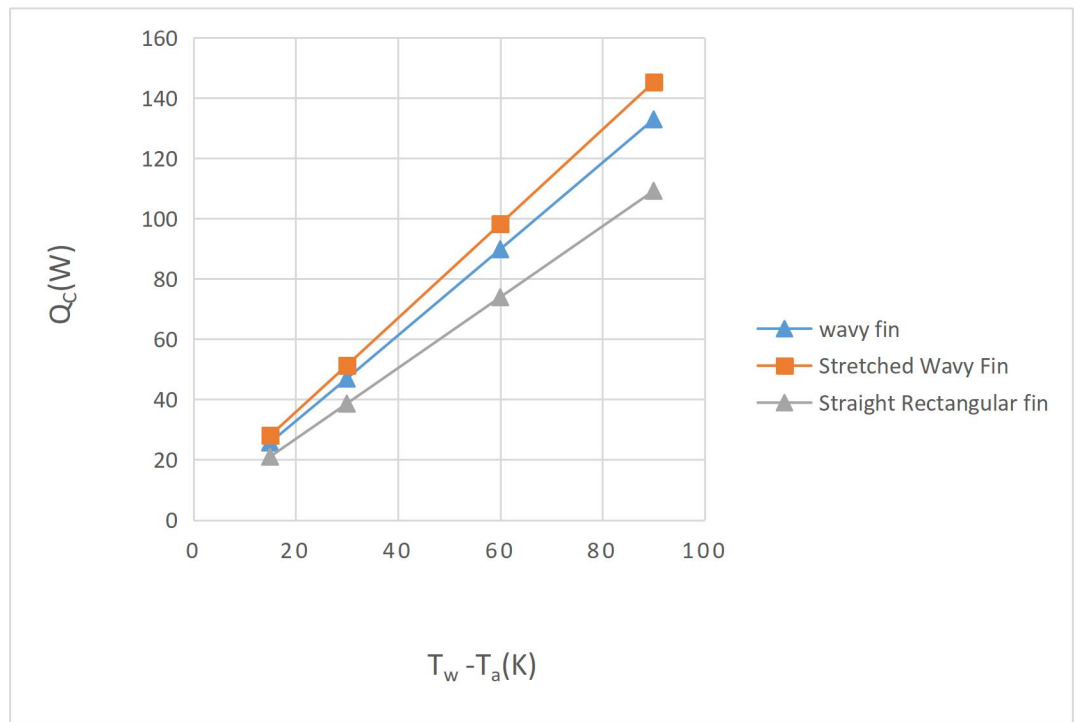


Figure 4.25: convective heat transfer Variation with base to ambient temperature difference for wavy fin, stretched wavy fin and straight rectangular fin

From Figure 4.24 it is observed that stretched wavy fin array into a straight rectangular fin array has the highest Convective heat transfer rate greater than the wavy fin array before it was stretched, by 9.25%, which is an insignificant percentage difference. It is also observed that the convective heat transfer rate for the wavy fin array is greater than that of the

straight rectangular fin array of the same fin height and fin spacing by about 28% at higher base-to-ambient temperature difference. This percentage difference can be considered reasonable. Though when also observed from the graph, at lower base-to-ambient temperature difference the convective heat transfer rate seems to be so close to each other. When the wavy fin effective or elliptical length was stretched into a straight fin, and their heat transfer rate compared, the stretched fin occupied additional height of about 43%. This implies that the use of a wavy fin array instead of the rectangular straight fin array eliminates fin additional space to the system design by 43%.

In conclusion, it is established from this study that wavy fin array possesses higher convection heat transfer performance than the straight rectangular fin array. Therefore in a bit to achieve high performance heat transfer with limited space a wavy fin array is recommended.

.CHAPTER FIVE

5.0. CONCLUSION AND RECOMMENDATION

5.1. Conclusion

This work presents the numerical simulation analysis of convective heat transfer rate of wavy fin array projecting from a horizontal rectangular base. Also a comparison of the rate of heat transfer was carried out with the rectangular straight fin array geometry and wavy fin array geometry, both of the same spacing the simulation results shows that;

The heat transfer rate increases as the height of the fin increases when compared with the base-to-ambient temperature difference.

The heat transfer rate of a wavy fin array when compared with the base-to-ambient temperature increases with decrease the in fin spacing. This is due to allowance for more increase in the number of fins.

The heat transfer rate from a wavy fin increases with decrease in wavelength of the fin irrespective of the other parameters considered. Therefore we can conclusively say that the heat transfer rate from any wavy fin array is dependent on the height of fin, spacing of fin, base-to-ambient temperature and the fin wavelength.

The straight rectangular fin array has been predominantly used as heat sink due to its high performance and low cost of machining. But when compared with the wavy fin it was discovered that wavy fin has a higher rate of heat transfer performance (about 28% higher), at the same fin height and spacing. When the wavy fin was stretched into a straight fin, and their heat transfer rate compared, the stretched fin occupied additional height of about 43%, which remains a problem of additional space and size of the any engineering system with

fin attachment, though had approximately 9% higher heat transfer rate than the original wavy geometry, which is insignificant if space must be conserved and size of the engineering system reduced. Based on the above premises, a wavy fin is best suitable for high heat transfer performance at conserved space and reduced size engineering systems.

5.2 Recommendation

At the conclusions of this work, it is recommended that further studies should be carried out to find out the heat transfer rate on wavy fin array protruding from a vertical base with varying number of perforations, as well as varying amplitude.

5.3 Contribution of Study to Knowledge

This study has actually made contribution to knowledge such that;

1. In the area of thermal engineering design of fins, this study has revealed that for effective heat transfer from engineering system with fin incorporation and system space conservation and reduced size, the wavy fin array geometry could be the best geometry. This is owing to the findings when the heat transfer rate of the wavy fin array was compared with the straight fin array of same length. It was discovered that the wavy had 28% heat transfer rate higher than the straight fin of the same fin height. When the wavy fin was stretched into a straight fin, and their heat transfer rate compared, the stretched fin occupied additional height of about 43%, which remains a problem of additional space and size of the any engineering system with fin attachment, though had approximately 9% higher heat transfer rate than the original

wavy geometry, which is insignificant if space must be conserved and size of the engineering system reduced.

2. Effect of the sinusoidal or wavy length of the wavy fin was also compared. A wavy fin of wavelength of 7mm was seen to have higher heat transfer rate, though much reduced effective fin length than the higher wavelength of 10mm. And this finding is of immense benefit to the thermal engineer when designing fins.

REFERENCES

- Bakale, R., Baheti, K., Dokade, C., & Galande, P. (2016). Experimental Analysis of Natural Convection Heat Transfer from Notched Fin. *Imperial Journal of interdisciplinary Reasearch* 2(6), 1211–1214.
- Bhambare, P. S., Kaithari, D. K., & Kharote, G. S. (2016). Fin Spacing Optimization for Isothermal Rectangular Polished Aluminum Fins on a Vertical Base, *International Journal of Scientific & Engineering Research*, 7(3 march, 2017).
- Bilir, L., & Ilken, Z. (2005). Effect of geometrical parameters on heat transfer and pressure drop characteristics of plate fin and tube heat exchangers, *Applied thermal Engineerint*, 25, 2421–2431. <https://doi.org/10.1016/j.applthermaleng.2004.12.019>
- Borrajopérez, R., & Reyes-fernández-de-bulnes, D. (2016). Thermal hydraulic performance of a wavy fin having two row of circular tubes Caracterización de una aleta ondulada con dos filas de tubos circulares, *Mechanical Engineering* 19(1), 1–9. Retrieved from <https://ingenieriamecanica.cujae.edu.cu/index.php/revistaim/article/view/528>
- Cuce, P. M., & Cuce, E. (2014). Optimization of configurations to enhance heat transfer from a longitudinal fin exposed to natural convection and radiation. *International Journal of Low-Carbon Technologies*, 305–310. <https://doi.org/10.1093/ijlct/ctt005>
- Dong, J., Zhang, Y., Li, G., & Xu, W. (2013). Fin optimization in heat sinks and Heat exchangers. *Journal of Thermal Energy Generation , Transport, Storage and Conversion*, 26(4), 384–396.
- Eastop, T. D., & McConkey, A. (2006). *Applied Thermodynamics for Engineering Technologies* (5th ed.). Pearson Education.
- Erbay, L. B., Doğan, B., & Öztürk, M. M. (2017). Comprehensive study of heat exchangers with louvered fins. *Heat Exchangers-Advanced Features and Applications*. Retrieved 15 September, 2019 from <http://www.intechopen/chapter/53343>. DOI: 10.5772/66472
- Incropera, F., Dewitt, D., Theodore, B., & Adrienne, L. (2007). *Fundamentals of Heat And mass Transfer* (6th ed.). United States of America: John Wiley & Sons, Inc. Retrieved from <http://www.wiley.com/go/permissions.%0A>To
- Kang, H. (2012). Evaluation of Fin Efficiency and Heat Transfer Coefficient for Fined Tube Heat Exchange. *International Journal of Engineering Research & Technology (IJERT)*, 3(7, NaN-2014).
- Khosravy, M. (n.d.). Extended Surfaces. <http://www.pdf.semanticscholar.org>

- Kim, Y. H., Kim, Y. C., & Kim, J. R. (2004). Effects of Fin and Tube Alignment on the Heat Transfer Performance of Finned-Tube Heat Exchangers with Large Fin Pitch. Layeni, A. T., Nwaokocha, C. N., Giwa, S. O., & Olamide, O. O. (2018). Numerical and Analytical Modeling of Solar for Chimney Combined Ventilation and Power in Buildings, 2(1).
- Lohar, G. P. (2014). Experimental Investigation for Optimizing Fin Spacing in Horizontal Rectangular Fin Array for Maximizing the Heat Transfer under a Natural and Forced Convection, *International Journal Of Engineering Research & Technology (IJERT)* Volume 03, Issue 07 (July 2014), 3(7), 1451–1453.
- Long, C., & Sayma, N. (2009). *Heat Transfer* (1st ed.). Retrieved from bookboon.com
- Lu, B. Y. Ğ., Yüncü, H., Mum, O. P. T. İ., Hesaplamak, A. Ğ. I., & İş, İ. Ç. İ. N. Y. E. N. İ. B. İ. R. E. Ş. İ. L. (2009). Rectangular Fin Arrays Subjected To Natural Convection Heat. *Journal. of Thermal Science and Technology*, 99–105.
- Mathiazhagan, P., & Jayabharathy, S. (2014). Heat transfer and temperature distribution of different fin geometry using numerical method heat transfer and temperature distribution of different fin geometry using numerical method. *Jp Journal of Heat and Mass Transfer*, 6, 223–234.
- May, P., & Almubarak, A. A. (2017). The Effects of Heat on Electronic Components, *International Journal of Engineering Research and Applications*, 7(5), 52–57. <https://doi.org/10.9790/9622-0705055257>
- Moorthy, P., Nicholas, N., & Oumer, A. N. (2018). Experimental Investigation on Effect of Fin Shape on the Thermal-Hydraulic Performance of Compact Fin-and-Tube Heat Exchangers. In *IOP Conference Series: Materials Science and Engineering PAPER*. <https://doi.org/10.1088/1757-899X/318/1/012070>
- Nikam, N. R., Pharate, G. M., & Tingare, S. V. (2015). Review on Heat Transfer Enhancement Using the Wavy Fin, *International Engineering Research Journal (IERJ)*, Special Issue Page 49-53, ISSN 2395-1621
- Pati, B., Sharma, B., Palo, A., & Barman, R. N. (2018). Numerical investigation of pin-fin thermal performance for staggered and inline arrays at low Reynolds number, *International Journal of Heat and Technology*, 36(2):697-703 DOI:10.18280/ijht.360235
- Rajput, R. (2003). *Heat and Mass Transfer* (3rd ed.). new delhi: s. chand & company.
- Senthil, R., Gupta, M., & Rath, C. (2017). Effect of fin spacing on forced convection heat transfer through the parabolic dish solar receiver, *Journal of Industrial Pollution Control*, 33(2), 1693–1698.
- Sharafian, A., mccague, C., & Bahrami, M. (2014). Impact of fin spacing on temperature distribution in adsorption cooling system for vehicle A / C applications. *International*

- Journal of Refrigeration*, 51, 135–143. <https://doi.org/10.1016/j.ijrefrig.2014.12.003>
- Miller, G. E. (1967). Optimum fin spacing for heat transfer per unit length of heat exchange section. Masters Thesis.5175. https://scholarsmine.mst.edu/masters_theses/5175
- Wolf, I., Frankovi, B., & Vili, I. (2006). A numerical and experimental analysis of heat transfer in a wavy fin-and-tube heat exchanger,*Energy and Environment*, 91–101.
- Yardi, A., Karguppikar, A., Tanksale, G., & Sharma, K. (2017). Optimization of Fin spacing by analyzing the heat transfer through rectangular fin array configurations (Natural convection). *International Research Journal of Engineering and Technology (IRJET)*, 4(09 september-2017), 985. Retrieved from www.irjet.com
- Yazicioğlu, B. (2005). *Performance of rectangular fins on a vertical base in free convection heat transfer*. Masters thesis, Middle East Technical University.

APPENDIX A

(Tables of Simulation results)

Table 1: Simulation Results at L=95 mm and W = 110 mm, $\lambda = 7$ mm

| H = 15 mm | | | | | | | | | | | |
|------------------|----------------|-----------------------------------|------------|----------------|-----------------------------------|-------------|----------------|-----------------------------------|-------------|----------------|-----------------------------------|
| S = 7.3 mm | | | S = 9.9 mm | | | S = 14.2 mm | | | S = 22.6 mm | | |
| Q | T _w | (T _w -T _a) | Q | T _w | (T _w -T _a) | Q | T _w | (T _w -T _a) | Q | T _w | (T _w -T _a) |
| (W) | (°C) | (°C) | (W) | (°C) | (°C) | (W) | (°C) | (°C) | (W) | (°C) | (°C) |
| 30.7 | 44.3 | 17.3 | 26.3 | 44.4 | 17.4 | 21.1 | 44.4 | 17.4 | 15.3 | 44.5 | 17.5 |
| 56.3 | 58.8 | 31.8 | 48.3 | 58.9 | 31.9 | 38.7 | 58.9 | 31.9 | 28.2 | 59.1 | 32.1 |
| 107.7 | 87.7 | 60.7 | 92.3 | 88.0 | 61.0 | 74.0 | 88.0 | 61.0 | 55.5 | 88.3 | 61.3 |
| 159.2 | 116.6 | 89.6 | 136.5 | 117.0 | 90 | 109.4 | 117.0 | 90 | 82.1 | 117.5 | 90.5 |
| H = 25 mm | | | | | | | | | | | |
| 34.9 | 44.3 | 17.3 | 29.7 | 44.3 | 17.3 | 23.4 | 44.4 | 17.4 | 18.3 | 44.4 | 17.4 |
| 63.2 | 58.7 | 31.7 | 54.5 | 58.8 | 31.8 | 43.0 | 58.8 | 31.8 | 35.5 | 59.0 | 32.0 |
| 120.7 | 87.4 | 60.4 | 104.3 | 87.7 | 60.7 | 82.2 | 87.8 | 60.8 | 64.1 | 88.0 | 61.0 |
| 178.6 | 116.2 | 89.2 | 154.3 | 116.6 | 89.6 | 121.5 | 116.7 | 89.7 | 94.9 | 117.1 | 90.1 |

| H = 35 mm | | | | | | | | | | | |
|-----------|-------|------|-------|-------|-------|-------|-------|------|-------|-------|------|
| 37.0 | 44.2 | 17.2 | 31.6 | 44.2 | 17.2 | 25.7 | 44.4 | 17.4 | 21.2 | 44.3 | 17.3 |
| 67.9 | 58.5 | 31.5 | 58.0 | 58.6 | 31.6 | 46.9 | 59.0 | 32.0 | 39.0 | 58.7 | 31.7 |
| 129.8 | 87.2 | 60.2 | 110.9 | 87.3 | 60.3 | 89.8 | 87.4 | 60.4 | 74.4 | 87.4 | 60.4 |
| 191.9 | 115.9 | 88.9 | 164.1 | 116.1 | 89.27 | 132.9 | 116.2 | 89.2 | 110.6 | 116.2 | 89.2 |

Table 2: Simulation Results At L=95 mm and W = 110 mm, $\lambda = 10$ mm

| H = 15 mm | | | | | | | | | | | |
|------------|------------------------|---|------------|------------------------|---|-------------|------------------------|---|-------------|------------------------|---|
| S = 7.3 mm | | | S = 9.9 mm | | | S = 14.2 mm | | | S = 22.6 mm | | |
| Q (W) | T _w (°C) | (T _w -T _a) (°C) | Q (W) | T _w (°C) | (T _w -T _a) (°C) | Q (W) | T _w (°C) | (T _w -T _a) (°C) | Q (W) | T _w (°C) | (T _w -T _a) (°C) |
| 22.32 | 44.79 | 17.79 | 13.28 | 44.90 | 17.9 | 11.84 | 44.88 | 17.88 | 8.99 | 44.90 | 17.9 |
| 35.86 | 59.67 | 32.67 | 24.40 | 59.75 | 32.74 | 21.68 | 59.77 | 32.77 | 16.53 | 59.81 | 32.81 |
| 63.02 | 89.42 | 62.42 | 46.72 | 89.52 | 62.52 | 44.43 | 89.55 | 62.55 | 31.67 | 89.64 | 62.64 |
| 90.3 | 119.2 | 92.2 | 69.1 | 119.3 | 92.3 | 61.3 | 119.4 | 92.4 | 46.9 | 119.5 | 92.5 |
| H = 25 mm | | | | | | | | | | | |

| | | | | | | | | | | | |
|-------|-------|-------|-------|--------|-------|-------|-------|-------|-------|-------|-------|
| 23.84 | 44.59 | 17.59 | 21.10 | 44.62 | 17.62 | 16.06 | 44.64 | 17.64 | 13.66 | 44.69 | 17.69 |
| 43.79 | 59.25 | 32.25 | 38.76 | 59.30 | 32.3 | 29.52 | 59.35 | 32.35 | 25.09 | 59.43 | 32.43 |
| 83.80 | 88.58 | 61.58 | 74.16 | 88.66 | 61.66 | 56.50 | 88.76 | 61.76 | 48.03 | 88.91 | 61.91 |
| 123.9 | 117.9 | 90.9 | 109.7 | 118.03 | 91.03 | 83.56 | 118.2 | 91.2 | 71.03 | 118.4 | 91.40 |

H = 35 mm

| | | | | | | | | | | | |
|-------|-------|-------|-------|--------|-------|-------|-------|-------|-------|-------|-------|
| 31.37 | 44.29 | 17.29 | 26.03 | 44.32 | 17.32 | 20.27 | 44.37 | 17.37 | 16.38 | 44.23 | 17.23 |
| 57.60 | 58.70 | 31.7 | 47.81 | 58.76 | 31.76 | 37.25 | 58.84 | 31.84 | 30.10 | 58.95 | 31.95 |
| 110.2 | 87.53 | 60.53 | 91.46 | 87.65 | 60.65 | 71.28 | 87.74 | 60.74 | 57.61 | 88.0 | 61 |
| 162.9 | 116.4 | 89.4 | 135.2 | 116.54 | 89.54 | 105.4 | 116.8 | 89.8 | 88.2 | 117.1 | 90.1 |

Table 3: Comparing the Heat Transfer Rate of Wavy and Straight Fin Array Length

| $T_w(^{\circ}\text{C})$ | $T_w - T_a(^{\circ}\text{C})$ | Wavy fin | Stretched wavy fin | Straight rectangular fin |
|-------------------------|-------------------------------|-----------------|--------------------|--------------------------|
| | | $Q_c(\text{W})$ | $Q_c(\text{W})$ | $Q_c(\text{W})$ |
| 45 | 15 | 25.7 | 28.0 | 21.0 |
| 60 | 30 | 46.9 | 51.3 | 38.6 |
| 90 | 60 | 89.8 | 98.2 | 73.9 |

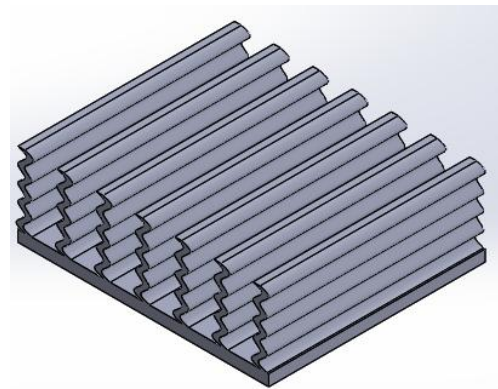
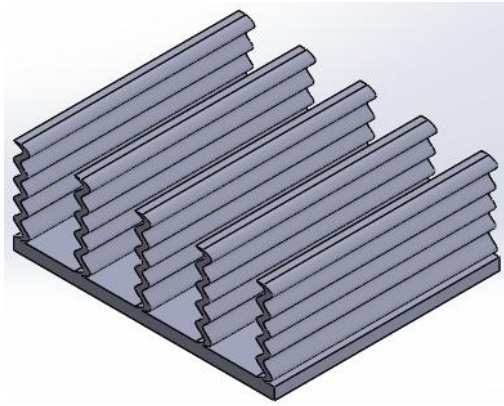
| | | | | |
|-----|----|-------|-------|-------|
| 120 | 90 | 132.9 | 145.2 | 109.2 |
|-----|----|-------|-------|-------|

Table 4: Result at $\Delta T = 150^{\circ}\text{C}$

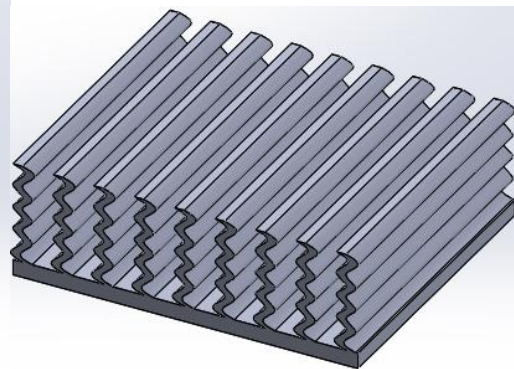
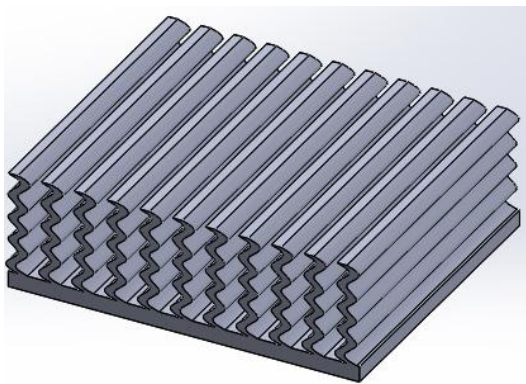
| No. of Fins | Heat transfer (W) | | % Error | Fin temperature ($^{\circ}\text{C}$) | | % Error |
|-------------|-------------------------|-------------------------|---------|--|-------------------------|---------|
| | $Q_{\text{experiment}}$ | $Q_{\text{simulation}}$ | | $T_{\text{experiment}}$ | $Q_{\text{simulation}}$ | |
| 4 | 6.66 | 6.75 | 1.35 | 48.00 | 49.82 | 3.79 |
| 5 | 8.93 | 8.67 | 2.99 | 45.90 | 49.80 | 8.5 |
| 6 | 8.85 | 8.20 | 7.34 | 46.00 | 49.80 | 8.26 |
| 8 | 8.33 | 8.25 | 0.96 | 49.3 | 49.70 | 1.01 |

APPENDIX B

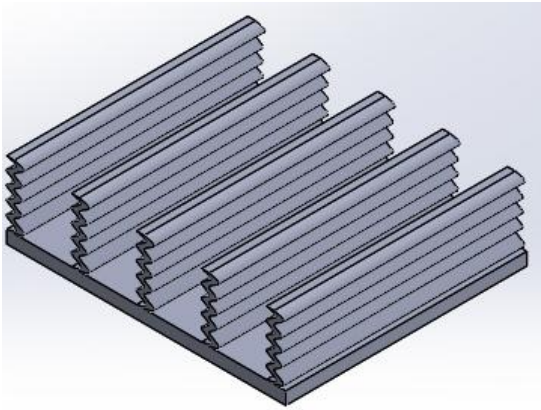
(Isometric models of fin configurations)



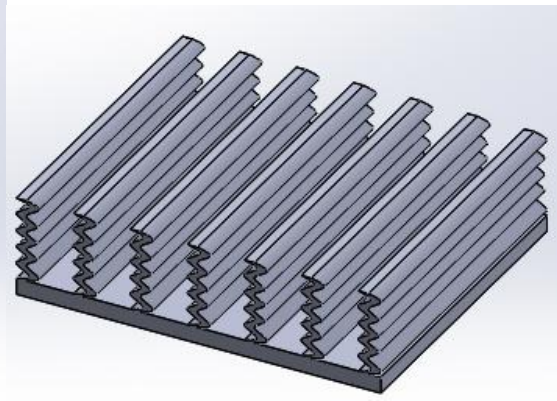
$H=35\text{ mm}, S=22.6\text{ mm}, \lambda=7\text{ mm}$ $H=35\text{ mm}, S=14.2\text{ mm}, \lambda=7\text{ mm}$



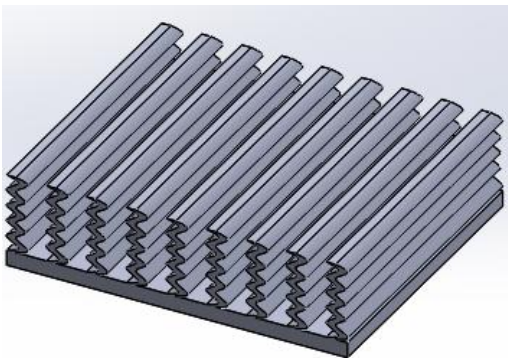
H= 35 mm, S= 7.3 mm, λ = 7 mm



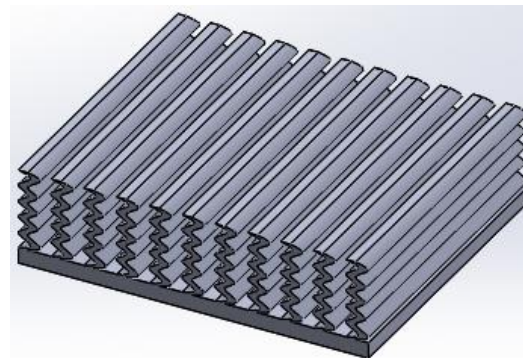
H= 35 mm, S= 9.9 mm, λ = 7 mm



H= 25 mm, S= 22.6 mm, λ = 7 mm

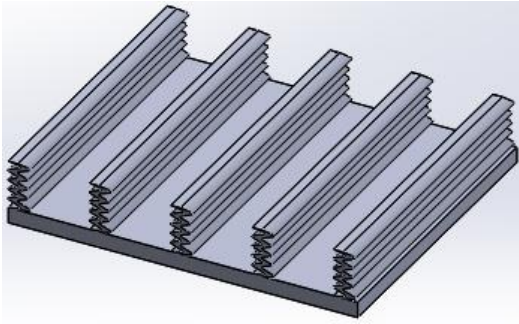


H= 25 mm, S= 14.2 mm, λ = 7 mm

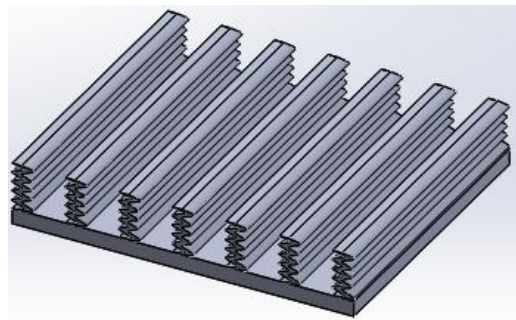


H= 25 mm, HS= 9.9 mm, 7 mm

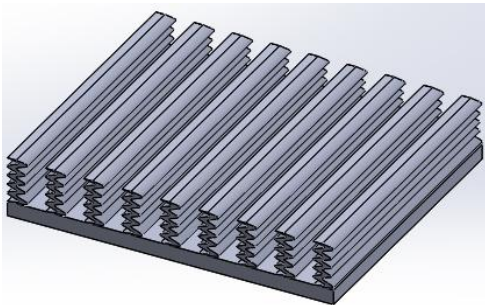
H= 25 mm, S= 7.3 mm, λ = 7 mm



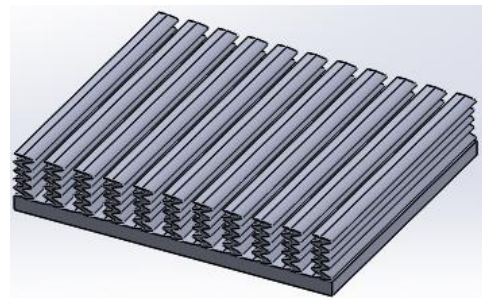
$H = 15 \text{ mm}, S = 22.6 \text{ mm}, \lambda = 7 \text{ mm}$



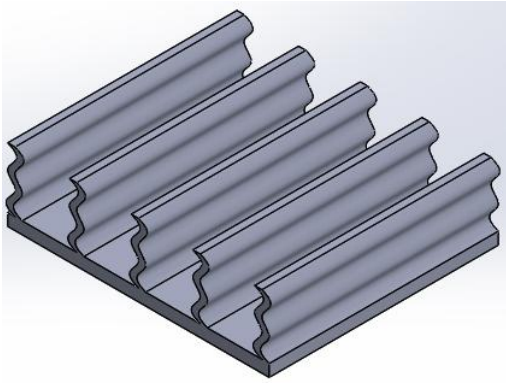
$H = 15 \text{ mm}, S = 14.2 \text{ mm}, \lambda = 7 \text{ mm}$



$H = 15 \text{ mm}, S = 9.9 \text{ mm}, \lambda = 7 \text{ mm}$

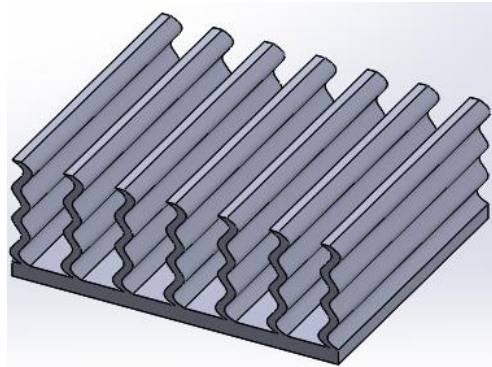


$H = 15 \text{ mm}, S = 7.3 \text{ mm}, \lambda = 7 \text{ mm}$

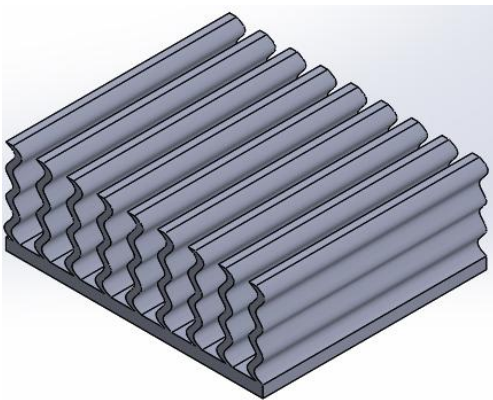


H=35 mm, S= 22.6 mm, λ = 10 mm

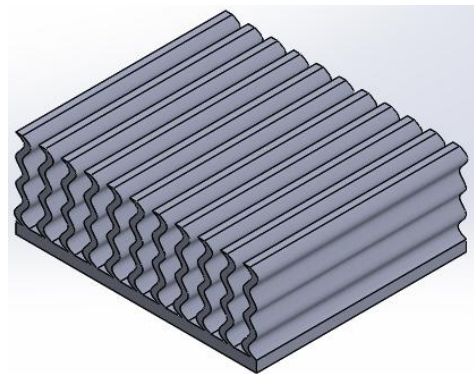
mm



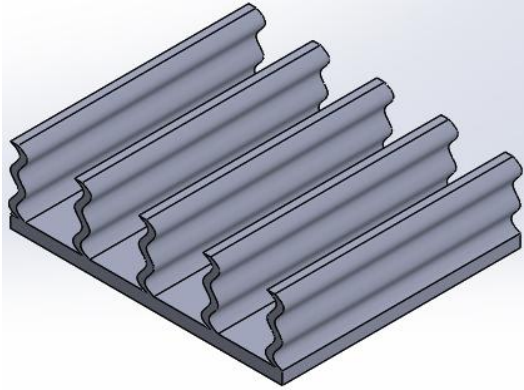
H=35 mm, S= 14.2 mm, λ = 10



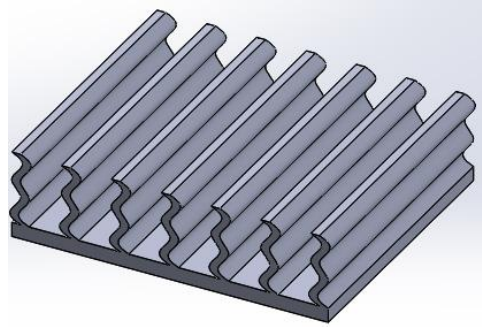
H=35 mm, S= 9.9 mm, λ =10 mm



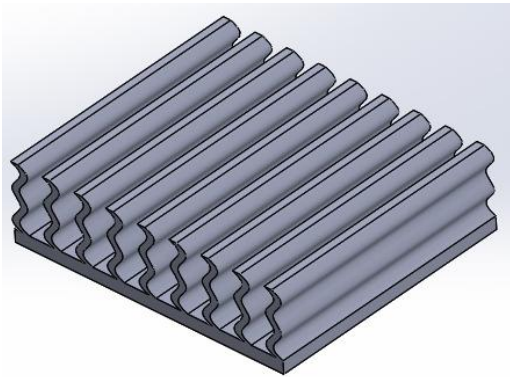
H=35 mm, S= 7.3 mm, λ = 10 mm



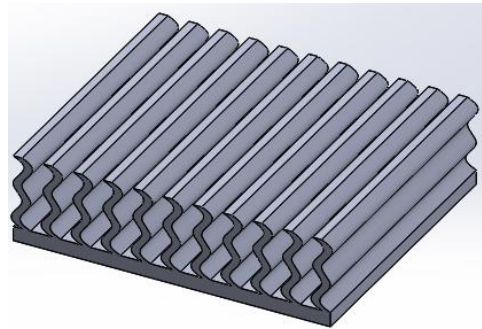
H=25 mm, S= 22.6 mm, $\lambda= 10$ mm



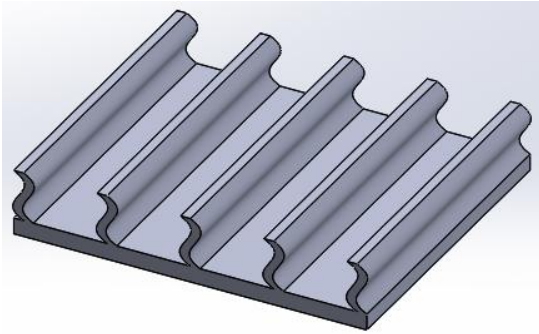
H=25 mm, S= 14.2 mm, $\lambda= 10$ mm



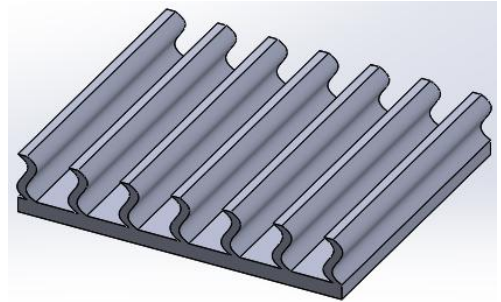
H=25 mm, S= 9.9 mm, $\lambda= 10$ mm



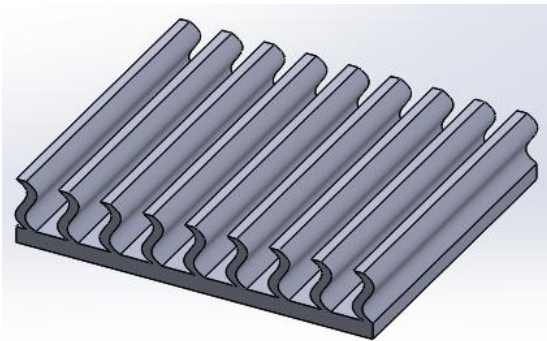
H=25 mm, S= 7.3 mm, $\lambda= 10$ mm



$H=15\text{ mm}$, $S=22.6\text{ mm}$, $\lambda=10\text{ mm}$

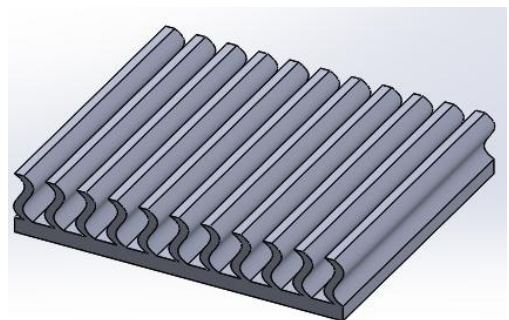


$H=15\text{ mm}$, $S=14.2\text{ mm}$, $\lambda=10\text{ mm}$

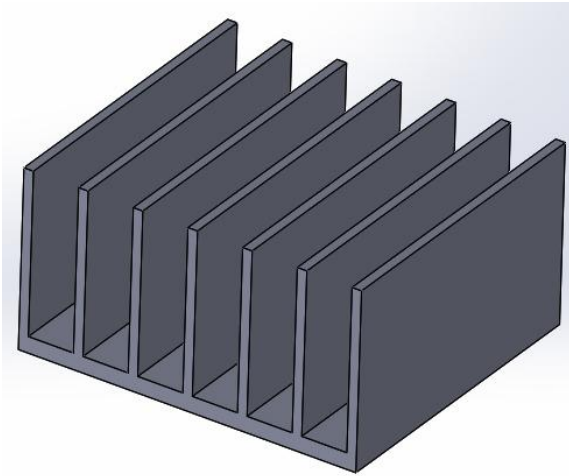


$H=15\text{ mm}$, $S=9.9\text{ mm}$, $\lambda=10\text{ mm}$

mm



$H=15\text{ mm}$, $S=7.3\text{ mm}$, $\lambda=10$



H=35 mm, S= 14.2 mm,